

# Photino and Gluino Production in SQED and SQCD

D.B. Espindola<sup>a</sup>, M. C. Rodriguez<sup>b</sup> and C. Brenner Mariotto<sup>b</sup>

<sup>a</sup>*Universidade Federal do Rio Grande do Sul*

*Instituto de Física - IF-UFRGS*

*Av. Bento Gonçalves, 9500*

*Caixa Postal 15051, Cep:91501-970,*

*Porto Alegre, RS*

*Brazil*

<sup>b</sup>*Universidade Federal do Rio Grande - FURG*

*Instituto de Matemática, Estatística e Física - IMEF*

*Av. Itália, km 8, Campus Carreiros*

*Caixa Postal 474, Cep:96201-900,*

*Rio Grande, RS*

*Brazil*

## Abstract

In this article we first present how to get Feynman amplitudes when we deal with Majorana fermions, based on a well defined fermion flow without explicit charge-conjugation matrices at vertices equations. We also present in detail the calculation for the production of photinos and gluinos.

PACS numbers: 12.60.-i 12.60.Jv 13.85.Lg

## 1 Introduction

Although the Standard Model (SM) [1], based on the gauge symmetry  $SU(3)_c \otimes SU(2)_L \otimes U(1)_Y$ , describes very well all the observed properties of charged leptons and quarks. Nevertheless, the SM is not considered as the ultimate theory since neither the fundamental parameters, masses and couplings, nor the symmetry pattern are predicted.

However, the necessity to go beyond it, from the experimental point of view, comes at the moment only from neutrino data. The recent groundbreaking discovery of nonzero neutrino masses and oscillations has put massive neutrinos as one of evidences on physics beyond the SM [2, 3, 4].

About the neutrino physics, one of the major problems is: Are the neutrinos Dirac or Majorana particles [5, 6, 7]? If neutrinos are Dirac particles, then lepton number remains as a conserved quantity. By another hand if neutrinos are Majorana particles, lepton number would be violated in two units [8]. In this case neutrinoless double beta decays and some rare meson decay of the form  $M^+ \rightarrow M'^- l^+ l^+$  can occur. This kind of decay is sensitive to neutrino masses and lepton mixing as discussed at [9]. Therefore, neutrino properties can play a crucial role in determining the matter-antimatter asymmetry of the universe if thermal leptogenesis is the correct solution to the baryogenesis problem [10, 11].

Supersymmetry (SUSY) arose in theoretical papers more than 30 years ago independently by Golfand and Likhtman [12], Volkov and Akulov [13] and Wess and Zumino [14]. On the first article [12] the authors found the superextension of the Poincaré algebra and constructed the first four-dimensional field theory with supersymmetry, (massive) quantum electrodynamics (SQED).

The particle content of SQED [15, 16, 17] is given by the electron (fermion), positron (antifermion) and the photon plus the spin 0 partners of electron and positrons, the so called selectron and spositron (sfermions). In this model we have also the photino, which is the spin (1/2) superpartner of the photon. One introduces the photon and the photino in the same vector superfield, due this fact the photino must be a Majorana fermion, because it satisfies the following constraint  $\lambda = \bar{\lambda}$ , see Eqs.(72,76) in Appendix A. In this theory both the  $R$ -Parity and chirality are conserved and sparticles appear in pairs at any vertex [15, 16, 17]. We present a brief review of this model at Appendix A.

We want to emphasize that the Minimal Supersymmetric Standard Model (MSSM) was constructed in 1975 [18, 19, 20], and the history of this model can be found at [21, 22]. On the earliest days of MSSM the “photon-neutrino”, now called as photino by short and its symbol is given by  $\tilde{\gamma}$ , was considered a fundamental particle, stable [23] and massless (at least at classical level) [24].

The gluino, in the earliest days, was called as “photonic neutrino” (the

gluino is denoted as  $\tilde{g}$ ). The gluino was thought as a massless particle, because it was difficult at that time to generate a sizeable mass for it. Being the fermion partner of the gluon (it is also Majorana fermion as the photino), its role and interactions are directly related with the properties of the supersymmetric QCD (SQCD) [15, 16] (See Appendix B for a short summary of the SQCD Feynman rules). Therefore, on the earliest day period, it was expected the existence of relatively light "*R*-hadrons"<sup>1</sup> [25, 26]. Today we know that a direct gaugino mass, its symbol is  $m_{1/2}$ , come from supergravity [27], or with a mass induced by radiative corrections using messenger quarks. Both mechanisms imply that the gluino masses are sufficiently heavy.

Today we know that SUSY can explain some phenomenological issues that the SM fails to address adequately [15, 16, 28, 29, 30, 31, 32]:

- Unification with gravity [33];
- Unification of Gauge Couplings [34];
- Hierarchy problem [35];
- Electroweak symmetry breaking (EWSB) [36];

These topics together the stability of the Lightest supersymmetric particle (LSP), from R-parity conservation [18], presumably a neutralino with interactions naturally of the order of weak-interaction, provides a very good Dark Matter candidate, is also a good point for SUSY [16, 28, 29, 30].

The studies about the photinos started in 1979 where P. Fayet [24] studied the interaction between photinos<sup>2</sup> with matter in the case where the photino is massless, obtaining the following cross section:

$$\sigma(\tilde{\gamma} + e^- \rightarrow \tilde{\gamma} + e^-) = \frac{4G_F^2 m_e E}{6\pi} \left( \frac{4M_W^2 \sin^2 \theta_W}{m_{s_e}^2} \right)^2, \quad (1)$$

where  $m_{s_e}$  is the mass of the slepton, see Ref. [22] for the old notation. With this article the phenomenological studies about photinos have started.

If the photino is stable, then all supersymmetric cascade decays end up decaying into photino. The photino leaves the detector unseen and its existence

---

<sup>1</sup>Particle made of quarks, antiquarks and gluinos

<sup>2</sup>In the MSSM context the photino is a more weakly interaction particle than the neutrino.

can only be inferred by looking for unbalanced momentum in a detector. In this way, they are phenomenologically similar to neutrinos, and they are not directly observable in particle detectors at accelerators. The events produced by the photinos are characterized by a large discrepancy in energy and momentum between the visible initial and final state particles. Nowadays this is the signal of the Lightest Supersymmetric Particle (LSP), which in some scenarios is the lightest neutralino ( $\tilde{\chi}_1^0$ ), the gravitino (the gravitino (symbol  $\tilde{G}$ ) is the supersymmetric partner of the graviton) or the lightest sneutrinos ( $\tilde{\nu}_1$ ).

Later in 1982 P. Fayet [37] get to photino production coming from  $e^-e^+$ , still in the case of massless photinos, with the following result

$$\frac{d\sigma}{d\Omega}(e^-e^+ \rightarrow \tilde{\gamma}\tilde{\gamma}) = \frac{\alpha^2 s}{16} \left[ \frac{(1 - \cos^2 \theta)^2}{\left(m_{s_e}^2 + \frac{s}{2}(1 - \cos^2 \theta)\right)^2} + \frac{(1 + \cos^2 \theta)^2}{\left(m_{t_e}^2 + \frac{s}{2}(1 + \cos^2 \theta)\right)^2} \right], \quad (2)$$

where  $\theta$  is the angle between the photino and the incoming electron as shown in Fig.(10). Later the calculus with a massive photino was done [38, 39]. The value of its mass  $M_{\tilde{\gamma}}$  assumed phenomenological importance due the fact it was related to the scale of supersymmetry breaking, as take place for the gluino today [23]. It is possible to show that gravity can induce Supersymmetry Breaking in such way that the photino is stable and its mass is a parameter given by[27]

$$M_{\tilde{\gamma}}^2 \sum m_{boson}^2 - \sum m_{fermion}^2 - N m_{gravitino}^2, \quad (3)$$

where  $N$  is a group factor, implying a possibly heavier photino mass. The total cross section in this case is given by [37]

$$\sigma(e^-e^+ \rightarrow \tilde{\gamma}\tilde{\gamma}) = \frac{2\pi\alpha^2 s}{3m_{s_e}^4}. \quad (4)$$

In this article, Ref. [37], Fayet also analysed the processes  $e^-e^+ \rightarrow \gamma\nu\bar{\nu}$  and  $e^-e^+ \rightarrow \gamma\tilde{\gamma}\tilde{\gamma}$  and obtained the following total cross sections (in  $pb$ )

$$\begin{aligned} \sigma(e^-e^+ \rightarrow \gamma\nu\bar{\nu}) &\approx 2.6 \cdot 10^{-2} \frac{s}{(40\text{GeV})^2}, \\ \sigma(e^-e^+ \rightarrow \gamma\tilde{\gamma}\tilde{\gamma}) &= 18 \left( \frac{m_{s_e}}{40\frac{\text{GeV}}{c^2}} \right)^{-4} \frac{s}{(40\text{GeV})^2}, \end{aligned} \quad (5)$$

The photino and selectron masses were included in these processes only in 1984 through the following Ref. [40, 41, 42]. At that time it was considered that these reactions could be a useful SUSY signature and these experiments could provide important limits on the photino and selectron masses. Two years later the reactions  $e^-e^+ \rightarrow \gamma\nu\bar{\nu}$  and  $e^-e^+ \rightarrow \gamma\tilde{\gamma}\tilde{\gamma}$  were calculated accurately, and they showed that the later process has bigger cross section compared with the first one (their Fig. 2), this holds only for the “lower” values of the selectron masses. They also showed that the processes with polarized and unpolarized beams are useful to put strong limits on the plane  $M_{\tilde{\gamma}} \times m_{\tilde{e}}$  (their Fig. 4) [43].

We also know that low-mass weakly interacting particles (photinos, neutrinos, axions, etc) are produced in hot astrophysical plasmas, and can thus transport energy out of stars. The possible astrophysical consequences of “light” photinos and gluinos, where the main photino production channel is the subprocess  $gg \rightarrow \tilde{g}\tilde{g}$  followed by a gluino (denoted as  $\tilde{g}$ ) decay  $\tilde{g} \rightarrow \tilde{\gamma}q\bar{q}$ , were discussed in [23, 44].

It has been generally assumed that for smaller values of gauginos masses the photino is an approximate eigenstate, but in general this is not the case. The classic signature of these events is missing transverse momentum ( $\cancel{p}_T$ ) from the escaping photinos, and this assumption was used by the UA1 Collaboration when doing their analysis [46].

Unfortunately, this approach can not be used to perform the data analyses of the Large Electron Positron Collider at European Organization for Nuclear Research (CERN LEP). In this case, for larger values of gaugino masses, it is not possible to think in terms of photino, zino and neutrals higgsinos ( $h_1^0$  and  $h_2^0$ ), but we need to consider the mixture of these states giving four neutralinos  $\tilde{\chi}_j^0$ ,  $j = 1, 2, 3, 4$ . In a similar way the mixing between the charged gauginos with the charged higgsinos give us two charginos  $\tilde{\chi}_i^\pm$ ,  $i = 1, 2$ . Now the dominant gluino decays are via  $\tilde{g} \rightarrow \bar{q}q\tilde{\chi}_i^\pm$  and  $\tilde{g} \rightarrow \bar{q}q\tilde{\chi}_i^0$  [16, 29, 46, 47].

About the rate of the two-body decay of the gluinos,  $\tilde{g} \rightarrow \tilde{\gamma}g$ , it was first analysed in Ref. [48], where it is noted that this decay rate vanishes if  $m_{\tilde{q}_L} = m_{\tilde{q}_R}$ . The partial width for the gluino radiative decay was recomputed (for  $m_{\tilde{\gamma}} = 0$ ) in Ref. [49] and by Barbieri *et al* in Ref. [50]. The most general result for the radiative decay width of the gluinos was calculated in Ref. [48] for the photino as the LSP [47]. Only for very massive gluinos ( $m_{\tilde{g}} > (m_q + m_{\tilde{q}})$ ) the two-body decays into quark plus squark become kinematically accessible and rapidly dominate the branching fraction [16, 29].

Supersymmetric theories involve self-conjugate Majorana spinors. Feynman rules for Majorana fermions, by another hand, involve vertices and propagators with clashing arrow. This is reflected by the appearance of the charge-conjugation matrix in Feynman rules for vertices and propagators, as appear at [16, 29, 30, 38]. In this approach the relative sign of interfering Feynman graphs cannot be read off the graphs, but has to be determined independently from the Wick contractions. This method is not so good to use in practical calculation as in photino and gluino production.

One of the goals of this article is to give a recipe, calculating the differential cross section of photino and gluino production, in order to get in an easy way the correct relative signs among different Feynmann diagrams for fermion-number-violating interactions. We review the mechanisms for producing the photinos in  $e^-e^+$  collisions for the International Linear Collider (ILC) [51], and also discuss the production of gluinos at the Large Hadron Collider (LHC) [52].

To get these production cross sections we review in Sec.(2) a simple way to write Feynman rules when dealing with Majorana particles, based on a well defined fermion flow, in a similar way as we do to get Feynman amplitudes for Dirac fermions. We review leptogenesis at Sec.(3), later at Secs.(4, 5) we present the details of the calculation to get the differential cross section of the production of photinos and gluinos, respectively. We point out that these processes can induce the matter-antimatter asymmetry. In Appendices (A,B) we present briefly the SQED and SQCD, respectively, while in Appendix (C) we give the mass spectrum of the sparticles used in this article.

## 2 Feynman Rules for Majorana Particles

Neutral particles might, or might not, have distinct antiparticles. Whereas the Dirac fermions have distinct antiparticles (the neutron is an example), in the case of Majorana fermions the reverse is true. Due this fact, a Majorana field  $\psi_M$  satisfies [38]

$$\psi_M = \psi_M^c \equiv C\bar{\psi}_M^T = C(\psi_M^\dagger\gamma^0)^T = C\gamma^0\psi_M^*, \quad (6)$$

where  $\bar{\psi} \equiv \psi^\dagger\gamma^0$  while  $C$  is the charge conjugation matrix defined as

$$C \equiv i\gamma^2\gamma^0, \quad (7)$$

which satisfies the following properties

$$\begin{aligned} C^\dagger &= C^{-1}, \\ C^T &= -C, \\ C^{-1}\Gamma_i C &= \eta_i \Gamma_i^T, \text{ for } \Gamma_i = 1, \gamma_5, \gamma_m \gamma_5, \gamma_m, \sigma_{m,n} = \frac{i}{2}[\gamma_m, \gamma_n], \end{aligned} \quad (8)$$

where  $\eta_i = +1$  for the first six  $\Gamma_i$  and  $\eta_i = -1$  for the last ten  $\Gamma_i$ . The  $\Gamma_i$  have been chosen such that

$$\Gamma_i^\dagger = \gamma^0 \Gamma_i \gamma^0. \quad (9)$$

In general, the  $u$  and  $v$  spinors for either Dirac or Majorana fermions are related via

$$\begin{aligned} u^{(s)}(k) &= C \bar{v}^{(s)T}(k), \\ v^{(s)}(k) &= C \bar{u}^{(s)T}(k), \end{aligned} \quad (10)$$

where  $s = \pm(1/2)$  labels spins.

In the SM [1] all the interactions conserve both Baryonic number ( $B$ ) and Leptonic number ( $L$ ). In contrast with the SM, the MSSM [18, 19, 20, 38] involve interactions that violate the fermion number, because this kind of models involve Majorana Fermions (do not have distinct antiparticles). Their self-conjugacy allows for a variety of different contractions, which acquire different signs originating from the anticommutativity of fermionic operators [38, 62, 63].

The usual Dirac field spinor expansion is given by [29]:

$$\Psi_D(x) = \int \frac{d^3k}{(2\pi)^3} \frac{1}{2E_{\vec{k}}} \sum_{s=\mp 1/2} \left[ c_{\vec{k},s} u^{(s)}(k) e^{-ikx} + d_{\vec{k},s}^\dagger v^{(s)}(k) e^{ikx} \right], \quad (11)$$

where  $c(c^\dagger)$  and  $d(d^\dagger)$  are annihilation (creation) operators satisfying

$$\begin{aligned} [c_{\vec{k},s}, c_{\vec{l},r}^\dagger] &= (2\pi)^3 2E_{\vec{k}} \delta_{sr} \delta^3(\vec{k} - \vec{l}), \quad [c_{\vec{k},s}, c_{\vec{l},r}] = [c_{\vec{k},s}^\dagger, c_{\vec{l},r}^\dagger] = 0, \\ [d_{\vec{k},s}, d_{\vec{l},r}^\dagger] &= (2\pi)^3 2E_{\vec{k}} \delta_{sr} \delta^3(\vec{k} - \vec{l}), \quad [d_{\vec{k},s}, d_{\vec{l},r}] = [d_{\vec{k},s}^\dagger, d_{\vec{l},r}^\dagger] = 0. \end{aligned} \quad (12)$$

The Dirac spinor field  $\Psi_D$  is quantized by require

$$\begin{aligned} \{\Psi_{Da}(x), \Psi_{Db}^\dagger(y)\} &= \delta_{ab} \delta^3(\vec{x} - \vec{y}), \\ \{\Psi_{Da}(x), \Psi_{Db}(y)\} &= \{\Psi_{Da}^\dagger(x), \Psi_{Db}^\dagger(y)\} = 0. \end{aligned} \quad (13)$$

Therefore for a Dirac spinor

$$\begin{aligned}\langle 0|T\{\Psi_{Da}(x)\bar{\Psi}_{Db}(y)\}|0\rangle &= S_{Fab}(x-y), \\ \langle 0|T\{\Psi_{Da}(x)\Psi_{Db}(y)\}|0\rangle &= \langle 0|T\{\bar{\Psi}_{Da}(x)\bar{\Psi}_{Db}(y)\}|0\rangle = 0.\end{aligned}\quad (14)$$

The similar expressions to the Majorana fermions [29] are given by:

$$\begin{aligned}\Psi_M(x) &= \int \frac{d^3k}{(2\pi)^3} \frac{1}{2E_{\vec{k}}} \sum_{s=\pm 1/2} [c_{\vec{k},s} u^{(s)}(k) e^{-ikx} + c_{\vec{k},s}^\dagger v^{(s)}(k) e^{ikx}], \\ [c_{\vec{k},s}, c_{\vec{l},r}^\dagger] &= (2\pi)^3 2E_{\vec{k}} \delta_{sr} \delta^3(\vec{k} - \vec{l}), \quad [c_{\vec{k},s}, c_{\vec{l},r}] = [c_{\vec{k},s}^\dagger, c_{\vec{l},r}^\dagger] = 0, \\ \langle 0|T\{\Psi_{Ma}(x)\bar{\Psi}_{Mb}(y)\}|0\rangle &= S_{Fab}(x-y), \\ \langle 0|T\{\Psi_{Ma}(x)\Psi_{Mb}(y)\}|0\rangle &= \langle 0|T\{\Psi_{Ma}(x)\bar{\Psi}_{Mc}(y)\}|0\rangle C_{cb}^T = S_{Fac}(x-y) C_{cb}^T, \\ \langle 0|T\{\bar{\Psi}_{Ma}(x)\bar{\Psi}_{Mb}(y)\}|0\rangle &= -\langle 0|T\{\Psi_{Mc}(x)\bar{\Psi}_{Mb}(y)\}|0\rangle C_{ca}^{-1} = -S_{Fcb}(x-y) C_{ca}^{-1},\end{aligned}\quad (15)$$

where  $c$  and  $c^\dagger$  are annihilation and creation operators<sup>3</sup>, and we must not forget to include these contractions when computing matrix elements of operators involving products of Majorana spinors fields [29, 38].

In general when we have one Dirac field we use the Feynman rules given at Fig.(1). For Majorana spinors, this rule appear ambiguous as there is no distinction between particle and antiparticle. Therefore, for Majorana fermion, there are three possibilities, see Eq.(15). These three possibilities are drawn at Fig.(2). Notice that the propagator have clashing arrows.

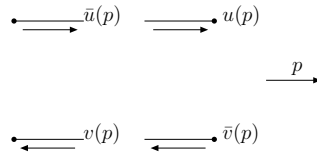


Figure 1: Feynman rules for an external Dirac fermion line.

---

<sup>3</sup>The condition  $c_{\vec{k},s} = d_{\vec{k},s}$  implies the identity of the particle and antiparticle quanta of this field.



$$\begin{aligned}
\beta \bullet \longrightarrow \alpha & \quad \left( \frac{i(\not{p} + m)}{p^2 - m^2 + i\epsilon} \right)_{\alpha\beta} \\
\beta \bullet \xrightarrow{p} \alpha & \quad \left( \frac{iC^{-1}(\not{p} + m)}{p^2 - m^2 + i\epsilon} \right)_{\alpha\beta} \\
\beta \bullet \xleftarrow{p} \alpha & \quad \left( \frac{-i(\not{p} + m)C}{p^2 - m^2 + i\epsilon} \right)_{\alpha\beta}
\end{aligned}$$

Figure 2: Feynmann rules for Majorana fermions propagators with orientation (thin arrow). The momentum  $p$  flows from left to right.

The most generic lagrangian  $\mathcal{L}$  for Majorana fields  $\lambda$  and Dirac fields  $\psi$ , as given by [38], augmented by a pure Dirac interaction term [62, 63], can be written in general formula in the following way

$$\begin{aligned}
\mathcal{L} = & \frac{1}{2} \bar{\lambda}_a (\not{\partial} - M_a) \lambda_a + \bar{\psi}_a (\not{\partial} - m_a) \psi_a + \frac{1}{2} g_{abc}^i \bar{\lambda}_a \Gamma_i \lambda_b \Phi_c \\
& + \frac{1}{2} g_{abc}^{i*} \bar{\lambda}_b \Gamma_i \lambda_a \Phi_c^* + \kappa_{abc}^i \bar{\lambda}_a \Gamma_i \psi_b \Phi_c^* + \kappa_{abc}^{i*} \bar{\psi}_b \Gamma_i \lambda_a \Phi_c + h_{abc}^i \bar{\psi}_a \Gamma_i \psi_b \Phi_c,
\end{aligned} \tag{16}$$

where  $\Gamma_i$  is defined at Eq.(8), and  $g_{abc}^i, \kappa_{abc}^i$  and  $h_{abc}^i$  are coupling constants. Some of the Feynman rules of this lagrangian were drawn at Fig.(3), the other Feynman rules are given at [38]. The field  $\Phi$  summarizes scalar and vector fields. Using Eq.(8) and the fact that fermion fields anticommute in the last term in the first line, we find that the following constraint must be satisfied

$$g_{abc}^i = \eta_i g_{bac}^i. \tag{17}$$

The second problem, as showed at [38], is the following. The last two terms in the first line of Eq.(16) can be rewritten as

$$\begin{aligned}
g_{abc}^i \bar{\lambda}_b \Gamma_i \lambda_a \Phi_c^* &= -g_{abc}^i \bar{\lambda}_a^T (C^{-1} \Gamma_i) \bar{\lambda}_b \Phi_c^*, \\
g_{abc}^i \bar{\lambda}_b \Gamma_i \lambda_a \Phi_c^* &= g_{abc}^i \bar{\lambda}_a (\Gamma_i C) \bar{\lambda}_b^T \Phi_c^*,
\end{aligned} \tag{18}$$

therefore the Feynman rules for this term are given by

$$i g_{abc}^i \Gamma_i,$$

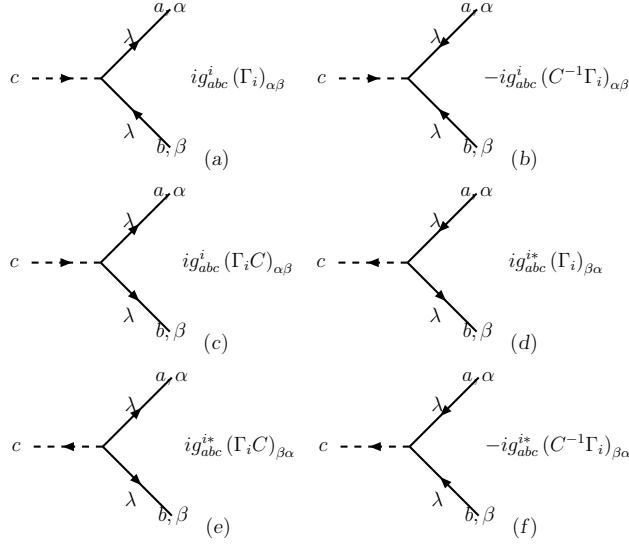


Figure 3: Feynmann rules for the interaction, from Eq.(16), of a scalar field with one Majorana ( $\lambda$ ) fermion taken from [38].

$$\begin{aligned}
& -ig_{abc}^i(C^{-1}\Gamma_i), \\
& ig_{abc}^i(\Gamma C),
\end{aligned} \tag{19}$$

these give the Feynman rules drawn at Fig.(3). The rules (a) and (e) are the usual ones, given by the first rule in the equation above. The rules (b) and (d) are given for the second vertices above while the last one are the (c) and (e) vertices.

We can also perform the following mathematical manipulations

$$ig_{abc}^i(\Gamma C)_{\alpha\beta} = ig_{abc}^i(\Gamma C)_{\beta\alpha}^T = -ig_{abc}^i(C\Gamma^T)_{\beta\alpha} = -i\eta_i g_{abc}^i(\Gamma C)_{\beta\alpha} \tag{20}$$

using Eq.(17) we get

$$ig_{abc}^i(\Gamma C)_{\alpha\beta} = -ig_{bac}^i(\Gamma C)_{\beta\alpha}, \tag{21}$$

which appears to be an evidence of a sign ambiguity [38].

This is reflected by the appearance of the charge-conjugation matrix in the Feynman rules for vertices and propagators, making it more complicated

to do calculations with them, and pretty far away from the rules for Dirac fermion. We have to stress that this method can be used without any problem, as shown at [38].

However, there is another way to define the Feynman rules for Majorana fermion. In this case, since the fermion flow is violated, one may introduce a continuous fermion flow orientation of each fermion line as done in Refs.[61, 62, 63]<sup>4</sup>. This forces one to introduce two analytical expressions for each vertex, one for fermion flow parallel, and one for fermion flow antiparallel to the flow of the fermion number. Therefore, for Majorana fermions there are only the usual spinors, see Fig.(4).

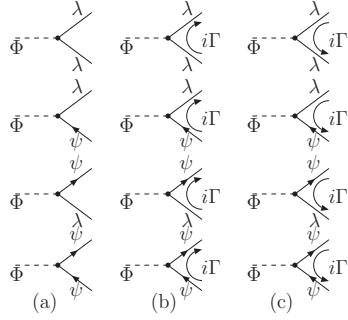


Figure 4: Feynmann rules for the interaction, from Eq.(16), of a scalar field with one Majorana ( $\lambda$ ) fermion taken from [62, 63].

The fermionic vertices are read off from the lagrangan as usual, but for every vertex containing fermions we need two expressions, the direct one ( $\Gamma$ ) and the reversed one ( $\Gamma'$ ). It is possible to reverse the interaction lagrangian introducing the charge-conjugate fields in the following way

$$\begin{aligned} g_{abc}^i \bar{\chi}_a \Gamma_i \chi_b \Phi_c &= g_{abc}^i (\bar{\chi}_a \Gamma_i \chi_b)^T \Phi_c = -g_{abc}^i \chi_b^T \Gamma_i^T \bar{\chi}_a^T \Phi_c = g_{abc}^i \bar{\chi}_b^c C \Gamma_i^T C^{-1} \chi_a^c \Phi_c \\ &= g_{abc}^i \bar{\chi}_b^c \eta_i \Gamma_i \chi_a^c \Phi_c, \end{aligned} \quad (22)$$

on the last stage we used Eq.(8). Therefore we have shown that

$$g_{abc}^i \bar{\chi}_a \Gamma_i \chi_b \Phi_c = g_{abc}^i \bar{\chi}_b^c \eta_i \Gamma_i \chi_a^c \Phi_c. \quad (23)$$

---

<sup>4</sup>We need only the familiar Dirac propagator and only vertices without explicit charge-conjugation matrices.

Therefore, if both the fermions are Majorana ones, we get Eq.(17) for all  $i$ . Due this fact we can rewrite the above equation, in general, as

$$\bar{\chi}\Gamma\chi = \bar{\chi}^c\Gamma'\chi^c, \quad (24)$$

and for Majorana fields holds the constraint

$$\Gamma = \Gamma'. \quad (25)$$

The Feynman amplitudes are obtained as follows [62, 63]:

1. Draw all possible Feynman diagrams for a given process;
2. Fix an arbitrary orientation (fermion flow) for each fermion chain;
3. Start at an external leg (for closed loops at some arbitrary propagator) and write down the Dirac matrices proceeding opposite to the chosen orientation (fermion flow) through the chain in agreement with Fig.(1);
4. Apply the corresponding analytical expressions in agreement with Fig.(4);
5. Multiply by a factor  $(-1)$  for every closed loop;
6. Multiply by the permutation parity of the spinors in the obtained analytical expression with the respect to some reference order;
7. As far as the determination of the combinatorial factor is concerned, Majorana fermions behave exactly like real scalar or vector fields.

In the book given at Ref.([64]), similar Feynman rules as given above are applied to Majorana fields (massive neutrinos) in Yukawa theory.

We can also use these Feynman rules to calculate the heavy right-handed neutrino decay, in this case we use leptogenesis to generate the baryon-antibaryon asymmetry of the universe (for more details about this subject we recomend the Refs. [10, 65]).

We want to stress that analytical expressions obtained using this recipe are independent of the choosen orientation. As a result of this fact, all sign ambiguities disappear and the relative sign of interfering Feynman diagrams is determined exactly as in the case of Dirac fermions. Another gain of this method is that the vertex expressions do not include explicit charge-conjugation matrices [62, 63].

This set of rules facilitates practical calculations, as we will show in next sections. Due this fact they were used together with the program FeynArts [66] in order to calculate the differential cross sections of the gluino production.

In general when we calculate the square amplitude involving Dirac fermions we use the following equations

$$\begin{aligned}\sum_s u^s(P)\bar{u}^s(P) &= (\not{P} + M), \\ \sum_s v^s(P)\bar{v}^s(P) &= (\not{P} - M).\end{aligned}\tag{26}$$

In diagrams involving Majorana fermions the formulas given at Eq.(26) remain valid, however, other combinations of the  $u$  and  $v$  spinors arise. Using Eq.(10), we can write the following relations

$$\begin{aligned}v^{(s)T} &= \bar{u}^{(s)}C^T, \quad u^{(s)T} = \bar{v}^{(s)}C^T, \\ \bar{u}^{(s)T} &= C^{-1}v^s, \quad \bar{v}^{(s)T} = C^{-1}u^s,\end{aligned}\tag{27}$$

using these new relations at Eq.(26) we get

$$\begin{aligned}\sum_s u^{(s)}(P)v^{(s)T}(P) &= \left(\sum_s u^{(s)}(P)\bar{u}^{(s)}(P)\right)C^T = (\not{P} + M)C^T, \\ \sum_s v^{(s)}(P)u^{(s)T}(P) &= \left(\sum_s v^{(s)}(P)\bar{v}^{(s)}(P)\right)C^T = (\not{P} - M)C^T, \\ \sum_s \bar{u}^{(s)T}(P)\bar{v}^{(s)T}(P) &= C^{-1}\left(\sum_s v^{(s)}(P)\bar{v}^{(s)}(P)\right) = C^{-1}(\not{P} - M), \\ \sum_s \bar{v}^{(s)T}(P)\bar{u}^{(s)T}(P) &= C^{-1}\left(\sum_s u^{(s)}(P)\bar{u}^{(s)}(P)\right) = C^{-1}(\not{P} + M),\end{aligned}\tag{28}$$

where  $C$  is the charge conjugation matrix which satisfy Eq.(8).

### 3 Leptogenesis

The mechanisms to create a baryon asymmetry from an initially symmetric state must in general satisfy the three basic conditions for baryogenesis as pointed out by Sakharov in 1967<sup>5</sup> [53]:

---

<sup>5</sup>They are known as Sakharov conditions

1. to violate baryon number,  $B$ ,
2. to violate  $C$  and  $CP$ , and
3. to be out of thermal equilibrium.

It is found that the  $CP$  violation observed in the quark sector [54] (e.g. in  $K^0$ - $\bar{K}^0$  or  $B^0$ - $\bar{B}^0$  mesons system) is far too small [55] to give rise to the observed baryon asymmetry, therefore these conditions are extended to include lepton number ( $L$ ) violation processes.

Within the class of renormalisable models that can give rise to the effective interaction to give mass to neutrinos, the type I seesaw mechanism [56] is perhaps the most elegant solution of all. Not only it can provide a way to generate tiny but nonzero neutrino masses, but also contains all the necessary ingredients for explaining the cosmic baryon asymmetry.

The idea of the type I seesaw model is quite simple. One introduces heavy neutral singlet fermions, the right-handed neutrinos (one for each generation of light neutrinos) in the SM, just as one would require to have a Dirac neutrino mass term. The  $SU(2)_L$  doublets  $l_\alpha = (\nu_L, e_L)_\alpha^T$ , where  $\alpha = 1, 2, 3$ , and  $\phi = (\phi^0, \phi^-)^T$  have their usual meanings. Using these fields, we get the following Lagrangian which is standard model gauge invariant:

$$-\mathcal{L} = Y_\nu \bar{l}_L \phi \nu_R + \frac{M_R}{2} \overline{(\nu_R)^c} \nu_R + \text{h.c.} , \quad (29)$$

where  $M_R$  denotes the bare mass for the right-handed neutrino. Since the SM does not predict or restrict the size of  $M_R$ , we may assume that it is arbitrarily large.

We can rewrite Eq.(29) in the following way

$$\mathcal{L}_\nu = -\frac{1}{2} \begin{pmatrix} \bar{\nu}_L & \overline{(\nu_R)^c} \end{pmatrix} \cdot \underbrace{\begin{pmatrix} 0 & m_D \\ m_D^T & M_R \end{pmatrix}}_M \cdot \begin{pmatrix} (\nu_L)^c \\ \nu_R \end{pmatrix} + \text{h.c.} , \quad (30)$$

where  $m_D \equiv Y_\nu \langle \phi^0 \rangle$ ,  $\nu_L \equiv (\nu_{1L}, \dots, \nu_{nL})^T$  and  $\nu_R \equiv (\nu_{1R}, \dots, \nu_{nR})^T$ .

So from this, it is easy to see that this model gives rise to two sets of Majorana neutrinos: the light ones ( $\nu$ ) with mass matrix  $m_\nu \simeq m_D M_R^{-1} m_D^T \equiv (\langle \phi^0 \rangle)^2 Y_\nu M_R^{-1} Y_\nu^T$ , and the heavy ones ( $N$ ) with  $M_N \simeq M_R$ . A particularly attractive feature of this is that the smallness of  $m_\nu$  is a direct consequence of

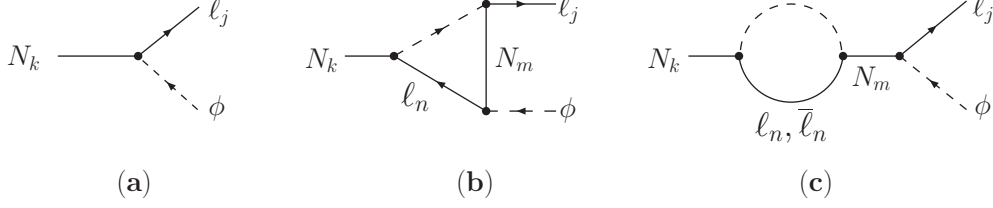


Figure 5: The **(a)** tree-level, **(b)** one-loop vertex correction, and **(c)** one-loop self-energy correction graphs for the decay:  $N_k \rightarrow l_j \bar{\phi}$ . This figure was taken from [10].

the large mass scale of  $M_R$ , which may have its origin from higher unification theories.

The classic leptogenesis scenario of Fukugita and Yanagida [57] involves taking the type I seesaw Lagrangian of Eq.(29), and the Yukawa coupling can then induce heavy right-handed neutrino (N) decays via two channels:

$$N_k \rightarrow \begin{cases} l_j + \bar{\phi}, \\ \bar{l}_j + \phi, \end{cases} \quad (31)$$

which violate lepton number by one unit. All Sakharov's conditions for leptogenesis will be satisfied if these decays also violate  $CP$  and go out of equilibrium at some stage during the evolution of the early universe. The requirement for  $CP$  violation means that the coupling matrix  $Y$  must be complex and the mass of  $N_k$  must be greater than the combined mass of  $l_j$  and  $\phi$ , so that interferences between the tree-level process (Fig. 5a) and the one-loop corrections (Fig. 5b, c) with on-shell intermediate states will be nonzero [10, 11].

But  $\phi$  is the scalar field of the SM. Therefore, we note that besides the tree-level interaction ( $N \leftrightarrow l\bar{\phi}$ ) of Fig. 5a, there are  $s$ -channel  $N\ell \leftrightarrow q_L\bar{t}_R$  (Fig. 6a) and  $t$ -channel  $Nt_R \leftrightarrow q_L\bar{\ell}$ ,  $Nq_L \leftrightarrow t_R\ell$  (Fig. 6b, c) scattering processes that can alter the abundance of  $N_1$ . For the evolution of  $B - L$ , in addition to these, there are also  $\Delta L = \pm 2$  scattering processes mediated by  $N_1$  (Fig. 7) which can be important.

It is important to remember that the SM can explain the conservation of lepton number (L) and of baryon number (B) without needing to impose any

discrete symmetry. However, this is not the case in supersymmetric theories, where to get all interactions to conserve L and B, we need to impose one discrete symmetry. This new symmetry is known as R-symmetry. The R-symmetry was introduced in 1975 by A. Salam and J. Strathdee and in an independent way by P. Fayet (see [58, 59] for a very nice review about this subject).

There is also the leptonic symmetry defined as

$$(Q, u^c, d^c) \rightarrow -(Q, u^c, d^c), (L, l^c, H_1, H_2) \rightarrow (L, l^c, H_1, H_2), \quad (32)$$

where the superpotential of the MSSM is given by:

$$\begin{aligned} W = & \mu \epsilon \hat{H}_1 \hat{H}_2 + \mu_{0a} \hat{L}_a \hat{H}_2 + f_{ab}^l \epsilon \hat{L}_a \hat{H}_1 \hat{l}_b^c + f_{ij}^u \epsilon \hat{Q}_i \hat{H}_2 \hat{u}_j^c + f_{ij}^d \epsilon \hat{Q}_i \hat{H}_1 \hat{d}_j^c \\ & + \lambda_{abc} \epsilon \hat{L}_a \hat{L}_b \hat{l}_c^c + \lambda'_{iaj} \epsilon \hat{Q}_i \hat{L}_a \hat{d}_j^c. \end{aligned} \quad (33)$$

The superpotential given above does not contain the  $\hat{u}\hat{d}\hat{d}$  term, which could induce the proton decay and also the neutron-antineutron oscillation, therefore the nucleon is stable in this model. However this superpotential allows and/or give contributions to the following nice processes [16, 29, 58, 59, 60]:

1. Double Beta Decay without Neutrinos
2. New contributions to the Neutrals  $K\bar{K}$  and also  $B\bar{B}$  Systems;
3. An additional contribution to the muon decay;
4. Charged Current Universality in  $\pi$  and  $\tau$  decays;
5. Charged Current Universality in the Quark Sector;
6. Leptonic Decays of Heavy Quarks Hadrons such as  $D^+ \rightarrow \bar{K}^0 l_i^+ \nu_i$ ;
7. Rare Leptonic Decays of Mesons like  $K^+ \rightarrow \pi^+ \nu \bar{\nu}$ ,
8. Hadronic  $B$  Meson Decay Asymmetries.



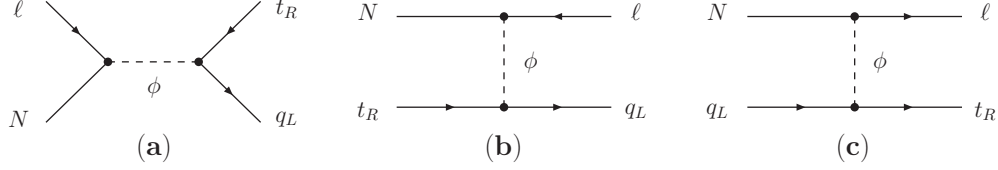


Figure 6: The  $\Delta L = \pm 1$  processes that can influence  $n_{N_1}$  and  $n_{B-L}$ : **(a)**  $s$ -channel scattering  $N\ell \leftrightarrow q_L \bar{t}_R$ , **(b)**  $t$ -channel scattering  $Nt_R \leftrightarrow q_L \bar{\ell}$ , **(c)**  $t$ -channel scattering  $Nq_L \leftrightarrow t_R \bar{\ell}$ . Here  $q_L$  denotes the 3rd generation of the quark doublet. This figure was taken from [10].

We want to stress that the third to the sixth points generate matter-antimatter asymmetry. We have the following direct decays of the lightest neutralinos

$$\begin{aligned}
\tilde{\chi}_1^0 &\rightarrow \bar{\nu}_a \bar{l}_b l_c, \quad \tilde{\chi}_1^0 \rightarrow \nu_a l_b \bar{l}_c, \quad \text{via } \lambda_{abc} \text{ coupling,} \\
\tilde{\chi}_1^0 &\rightarrow l_a^+ \bar{u}_j d_i, \quad \tilde{\chi}_1^0 \rightarrow l_a^- u_j \bar{d}_i, \quad \text{via } \lambda'_{iaj} \text{ coupling,} \\
\tilde{\chi}_1^0 &\rightarrow \bar{\nu}_a \bar{d}_j d_i, \quad \tilde{\chi}_1^0 \rightarrow \nu_a d_j \bar{d}_i, \quad \text{via } \lambda'_{iaj} \text{ coupling,}
\end{aligned} \tag{34}$$

and for lightest charginos (only via  $\lambda'_{iaj}$  coupling)

$$\begin{aligned}
\tilde{\chi}_1^+ &\rightarrow l_i^+ \bar{d}_j d_k, \quad \tilde{\chi}_1^+ \rightarrow l_i^+ \bar{u}_j u_k, \\
\tilde{\chi}_1^+ &\rightarrow \bar{\nu}_i \bar{d}_j u_k, \quad \tilde{\chi}_1^+ \rightarrow \nu_i u_j \bar{d}_k.
\end{aligned} \tag{35}$$

On the next section we will present a process of the type  $e^- e^+ \rightarrow \tilde{\gamma} \tilde{\gamma}$ , which is the basic step if we want to calculate the following processes<sup>6</sup>:  $e_L^- + e_L^- \rightarrow \tilde{\chi}_i^- \tilde{\chi}_i^- \rightarrow \mu^- + \mu^- + \text{jets}$ ,  $e_L^- + e_L^- \rightarrow \tilde{\chi}_i^- \tilde{\chi}_i^- \rightarrow e^- + \mu^- + \text{jets}$ ,  $e_L^- + e_L^- \rightarrow \tilde{\chi}_i^- \tilde{\chi}_i^- \rightarrow \mu^- + \mu^- + \text{jets}$ ,  $e_L^- + e_L^- \rightarrow \tilde{\chi}_i^- \tilde{\chi}_i^- \rightarrow \tau^- + \mu^- + \text{jets}$  or  $e_L^- + e_L^- \rightarrow \tilde{\chi}_i^- \tilde{\chi}_i^- \rightarrow \tau^- + \tau^- + \text{jets}$ . These processes can generate leptogenesis in this model.

## 4 Photino Production

The goal of this section is to present explicitly how to calculate the differential cross section of the process  $e^- e^+ \rightarrow \tilde{\gamma} \tilde{\gamma}$ , in the SQED context, this process

---

<sup>6</sup>Due the  $\lambda_{abc}$  coefficient.

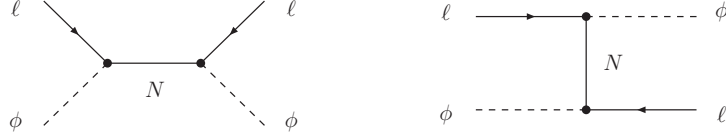


Figure 7: The  $\Delta L = \pm 2$   $s$ - and  $t$ -channel scattering processes mediated by  $N$ . This figure was taken from [10].

violate lepton number by two unit. In this case it takes place via  $t$ -channel  $\tilde{e}_L^-$ - and  $\tilde{e}_R^-$ -exchange, see Fig.(8), as shown by Fayet in his article [37]. Note that both  $e$  and  $\tilde{e}$  carry one unit of lepton number. The  $t$ -channel and  $u$ -channel exchanges correspond to the cases where the fermion lines are uncrossed and crossed, respectively. These are analogous to the  $t$ -channel and  $u$ -channel diagrams in  $e^-e^+ \rightarrow \gamma\gamma$ , where in this case an electron is exchanged (see Fig.(9)). On the later we have only two diagrams because  $e_L = e_R$ , while in the SQED (the same is hold in the MSSM)  $\tilde{e}_L \neq \tilde{e}_R$  and then we have four diagrams for the process  $e^-e^+ \rightarrow \tilde{\gamma}\tilde{\gamma}$ .

Today we know that, in the context of the MSSM, the photino is a gaugino and it mixes with the neutral higgsinos to give the neutralinos as mass eigenstates [16, 29, 67]. Neutralino pair production in  $e^-e^+$  collisions was first studied in [68], where it was shown that this production takes place via the  $s$ -channel  $Z$ -exchange and  $t$ -channel  $\tilde{e}_L^-$ - and  $\tilde{e}_R^-$ -exchange. The corresponding expressions for the differential cross sections are showed in Appendix A of the reference [29]. By another hand, the “Lighest supersymmetric particle” (LSP) in some minimal Supergravity (mSUGRA) scenarios can be a light photino (it means  $\tilde{\chi}_1^0 \approx \tilde{\gamma}$ ) [69, 70, 71] with an acceptable cosmological abundance [72].

In  $e^-e^+$  collisions, photinos are produced in the following reaction

$$e^-(P_1) + e^+(P_2) \rightarrow \tilde{\gamma}(K_1) + \tilde{\gamma}(K_2) \quad (36)$$

as shown in Fig.(10), where  $\tilde{\gamma}$  is the photino, and the particle four-momenta are specified in parentheses. It is important to stress that the photino is its own antiparticle. The amplitudes for  $e^-(P_1)e^+(P_2) \rightarrow \tilde{\gamma}(K_1)\tilde{\gamma}(K_2)$  are:

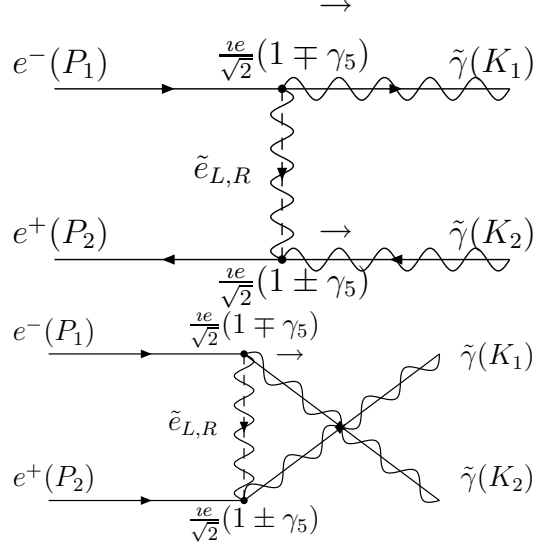


Figure 8: Feynmann diagram to the process  $e^-e^+ \rightarrow \tilde{\gamma}\tilde{\gamma}$ , we fix the orientation (fermion flow) for each lepton as given by the electron, therefore the positron line have opposite direction, in such way we get a continuous line in the diagram.

$$\begin{aligned}
\mathcal{M}_a &= -\frac{e^2}{2} \bar{u}(K_1)(1 - \gamma_5)u(P_1) \frac{1}{t - M_{\tilde{e}_L}^2} \bar{v}(P_2)(1 + \gamma_5)v(K_2), \\
\mathcal{M}_b &= -\frac{e^2}{2} \bar{u}(K_1)(1 + \gamma_5)u(P_1) \frac{1}{t - M_{\tilde{e}_R}^2} \bar{v}(P_2)(1 - \gamma_5)v(K_2), \\
\mathcal{M}_c &= \frac{e^2}{2} \bar{u}(K_2)(1 - \gamma_5)u(P_1) \frac{1}{u - M_{\tilde{e}_L}^2} \bar{v}(P_2)(1 + \gamma_5)v(K_1), \\
\mathcal{M}_d &= \frac{e^2}{2} \bar{u}(K_2)(1 + \gamma_5)u(P_1) \frac{1}{u - M_{\tilde{e}_R}^2} \bar{v}(P_2)(1 - \gamma_5)v(K_1), \quad (37)
\end{aligned}$$

where  $s, t, u$  are the Mandelstam variables defined as

$$\begin{aligned}
s &= (P_1 + P_2)^2 = (K_1 + K_2)^2, \\
t &= (P_1 - K_1)^2 = (P_2 - K_2)^2, \\
u &= (P_1 - K_2)^2 = (P_2 - K_1)^2. \quad (38)
\end{aligned}$$

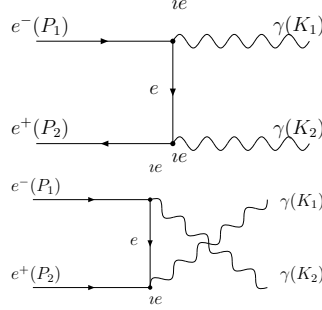


Figure 9: Feynmann diagram to the process  $e^-e^+ \rightarrow \gamma\gamma$ , in this case we have only 2 diagrams against the 4 in  $e^-e^+ \rightarrow \tilde{\gamma}\tilde{\gamma}$  scattering, see Fig.(8).

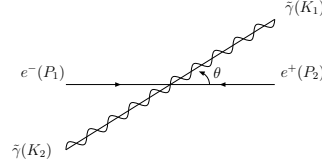


Figure 10: Kinematics of the process  $e^-e^+ \rightarrow \tilde{\gamma}\tilde{\gamma}$  in the center of mass frame, only Dirac fermions have lepton lines with orientation from left to right for the electrons and of course opposite orientation for the positron. The photinos are Majorana particles and due to this fact we can not fix an orientation to the flow.

The next step is to calculate  $|\mathcal{M}_a + \mathcal{M}_b - \mathcal{M}_c - \mathcal{M}_d|^2$ , where the relative minus sign arise due to Pauli statistic. Summing over initial and final spins and using the usual Projection Operator over the positive and negative energy states we get (see [73] for more details on the algebraic manipulations) the following expressions

$$|\mathcal{M}_a|^2 = \frac{16e^4}{(t - M_{\tilde{e}_L}^2)^2} (P_1 \cdot K_1)(P_2 \cdot K_2) = \frac{4e^4}{(t - M_{\tilde{e}_L}^2)^2} (t - m_e^2 - M_{\tilde{\gamma}}^2)^2,$$

$$\mathcal{M}_a^\dagger \mathcal{M}_b = \mathcal{M}_b \mathcal{M}_c^\dagger = \frac{e^4}{4(t - M_{\tilde{e}_L}^2)(t - M_{\tilde{e}_R}^2)} (8m_e M_{\tilde{\gamma}})^2,$$

$$\begin{aligned}
|\mathcal{M}_b|^2 &= \frac{16e^4}{(t - M_{\tilde{e}_R}^2)^2} (P_1 \cdot K_1)(P_2 \cdot K_2) = \frac{4e^4}{(t - M_{\tilde{e}_R}^2)^2} (t - m_e^2 - M_{\tilde{\gamma}}^2)^2, \\
|\mathcal{M}_c|^2 &= \frac{16e^4}{(u - M_{\tilde{e}_L}^2)^2} (P_1 \cdot K_2)(P_2 \cdot K_1) = \frac{4e^4}{(u - M_{\tilde{e}_L}^2)^2} (u - m_e^2 - M_{\tilde{\gamma}}^2)^2, \\
|\mathcal{M}_d|^2 &= \frac{16e^4}{(u - M_{\tilde{e}_R}^2)^2} (P_1 \cdot K_2)(P_2 \cdot K_1) = \frac{4e^4}{(u - M_{\tilde{e}_R}^2)^2} (u - m_e^2 - M_{\tilde{\gamma}}^2)^2.
\end{aligned} \tag{39}$$

Lets work out the interference terms in detail. On this case we need again to sum over initial and final spins and using Eqs.(26,28) we get the following results

$$\begin{aligned}
\mathcal{M}_a^\dagger \mathcal{M}_c &= \mathcal{M}_c^\dagger \mathcal{M}_a = \frac{e^4}{4(u - M_{\tilde{e}_L}^2)(t - M_{\tilde{e}_L}^2)} \{ \text{Tr} [(1 + \gamma_5)(\not{P}_1 + m_e)(1 - \gamma_5)) \\
&\quad \cdot (\not{K}_1 + M_{\tilde{\gamma}})C^T(1 - \gamma_5)^T(\not{P}_2 - m_e)^T(1 + \gamma_5)^TC^{-1}(\not{K}_2 + M_{\tilde{\gamma}})] \}, \\
\mathcal{M}_a^\dagger \mathcal{M}_d &= \mathcal{M}_d^\dagger \mathcal{M}_a = \frac{e^4}{4(t - M_{\tilde{e}_L}^2)(u - M_{\tilde{e}_R}^2)} \{ \text{Tr} [(1 + \gamma_5)(\not{P}_1 + m_e)(1 + \gamma_5)) \\
&\quad \cdot (\not{K}_1 + M_{\tilde{\gamma}})C^T(1 - \gamma_5)^T(\not{P}_2 - m_e)^T(1 - \gamma_5)^TC^{-1}(\not{K}_2 + M_{\tilde{\gamma}})] \}, \\
\mathcal{M}_b^\dagger \mathcal{M}_c &= \mathcal{M}_c^\dagger \mathcal{M}_b = \frac{e^4}{4(t - M_{\tilde{e}_L}^2)(u - M_{\tilde{e}_R}^2)} \{ \text{Tr} [(1 + \gamma_5)(\not{P}_1 + m_e)(1 + \gamma_5)) \\
&\quad \cdot (\not{K}_1 + M_{\tilde{\gamma}})C^T(1 - \gamma_5)^T(\not{P}_2 - m_e)^T(1 - \gamma_5)^TC^{-1}(\not{K}_2 + M_{\tilde{\gamma}})] \}, \\
\mathcal{M}_b^\dagger \mathcal{M}_d &= \mathcal{M}_d^\dagger \mathcal{M}_b = \frac{e^4}{4(u - M_{\tilde{e}_R}^2)(t - M_{\tilde{e}_R}^2)} \{ \text{Tr} [(1 + \gamma_5)(\not{P}_1 + m_e)(1 - \gamma_5)) \\
&\quad \cdot (\not{K}_1 + M_{\tilde{\gamma}})C^T(1 - \gamma_5)^T(\not{P}_2 - m_e)^T(1 + \gamma_5)^TC^{-1}(\not{K}_2 + M_{\tilde{\gamma}})] \}, \\
\mathcal{M}_c^\dagger \mathcal{M}_d &= \mathcal{M}_c^\dagger \mathcal{M}_d = \frac{e^4}{4(t - M_{\tilde{e}_L}^2)(u - M_{\tilde{e}_R}^2)} \{ \text{Tr} [(1 + \gamma_5)(\not{P}_1 + m_e)(1 + \gamma_5)) \\
&\quad \cdot (\not{K}_1 + M_{\tilde{\gamma}})C^T(1 - \gamma_5)^T(\not{P}_2 - m_e)^T(1 - \gamma_5)^TC^{-1}(\not{K}_2 + M_{\tilde{\gamma}})] \},
\end{aligned} \tag{40}$$

Using Eq.(8) we can show in a simple way that

$$\begin{aligned}
C^T(1 - \gamma_5)^T(\not{P}_2 - m_e)^T(1 - \gamma_5)^TC^{-1} &= (1 + \gamma_5)(\not{P}_2 + m_e)(1 + \gamma_5), \\
C^T(1 - \gamma_5)^T(\not{P}_2 - m_e)^T(1 + \gamma_5)^TC^{-1} &= (1 - \gamma_5)(\not{P}_2 + m_e)(1 + \gamma_5).
\end{aligned} \tag{41}$$

Now using the trace techniques we get

$$\begin{aligned}
\mathcal{M}_a^\dagger \mathcal{M}_c &= \mathcal{M}_c^\dagger \mathcal{M}_a = \frac{8e^4 M_{\tilde{\gamma}}^2}{(u - M_{\tilde{e}_L}^2)(t - M_{\tilde{e}_L}^2)} (P_1 \cdot P_2), \\
&= \frac{8e^4 M_{\tilde{\gamma}}^2}{(u - M_{\tilde{e}_L}^2)(t - M_{\tilde{e}_L}^2)} \left( \frac{s}{2} - m_e^2 \right), \\
\mathcal{M}_a^\dagger \mathcal{M}_d &= \mathcal{M}_d^\dagger \mathcal{M}_a = \frac{e^4}{4(t - M_{\tilde{e}_L}^2)(u - M_{\tilde{e}_R}^2)} (8m_e M_{\tilde{\gamma}})^2, \\
\mathcal{M}_b^\dagger \mathcal{M}_c &= \mathcal{M}_c^\dagger \mathcal{M}_b = \frac{e^4}{4(t - M_{\tilde{e}_R}^2)(u - M_{\tilde{e}_L}^2)} (8m_e M_{\tilde{\gamma}})^2, \\
\mathcal{M}_b^\dagger \mathcal{M}_d &= \mathcal{M}_d^\dagger \mathcal{M}_b = \frac{8e^4 M_{\tilde{\gamma}}^2}{(u - M_{\tilde{e}_R}^2)(t - M_{\tilde{e}_R}^2)} (P_1 \cdot P_2), \\
&= \frac{8e^4 M_{\tilde{\gamma}}^2}{(u - M_{\tilde{e}_R}^2)(t - M_{\tilde{e}_R}^2)} \left( \frac{s}{2} - m_e^2 \right), \\
\mathcal{M}_c^\dagger \mathcal{M}_d &= \mathcal{M}_d^\dagger \mathcal{M}_c = \frac{e^4}{4(u - M_{\tilde{e}_R}^2)(u - M_{\tilde{e}_L}^2)} (8m_e M_{\tilde{\gamma}})^2. \tag{42}
\end{aligned}$$

Therefore the differential cross section, in the limit  $M_{\tilde{e}_L}^2 = M_{\tilde{e}_R}^2 = M_{\tilde{e}}^2$ , is given by

$$\begin{aligned}
\frac{d\sigma}{d\Omega}(e^- e^+ \rightarrow \tilde{\gamma} \tilde{\gamma}) &= \frac{\alpha^2}{4s} \sqrt{\frac{s - 4M_{\tilde{\gamma}}^2}{s - 4m_e^2}} \left[ \left( \frac{t - M_{\tilde{\gamma}}^2 - m_e^2}{t - M_{\tilde{e}}^2} \right)^2 + \left( \frac{u - M_{\tilde{\gamma}}^2 - m_e^2}{u - M_{\tilde{e}}^2} \right)^2 \right. \\
&\quad \left. + \left( \frac{2m_e M_{\tilde{\gamma}}}{t - M_{\tilde{e}}^2} \right)^2 + \left( \frac{2m_e M_{\tilde{\gamma}}}{u - M_{\tilde{e}}^2} \right)^2 + \left( \frac{16m_e^2 M_{\tilde{\gamma}}^2 - 2s M_{\tilde{\gamma}}^2}{(t - M_{\tilde{e}}^2)(u - M_{\tilde{e}}^2)} \right) \right]. \tag{43}
\end{aligned}$$

Since the photino is not actually a mass eigenstate (remember that our calculation is done in the context of sQED), we have used the neutralino masses for the photino. In any case, the electron mass could be neglected compared with the sparticle masses, and the expression above simplifies to

$$\begin{aligned}
\frac{d\sigma}{d\Omega}(e^- e^+ \rightarrow \tilde{\gamma} \tilde{\gamma}) &= \frac{\alpha^2}{4s} \sqrt{1 - \left( \frac{2M_{\tilde{\gamma}}}{\sqrt{s}} \right)^2} \left[ \left( \frac{t - M_{\tilde{\gamma}}^2}{t - M_{\tilde{e}}^2} \right)^2 + \left( \frac{u - M_{\tilde{\gamma}}^2}{u - M_{\tilde{e}}^2} \right)^2 \right. \\
&\quad \left. - \frac{2s M_{\tilde{\gamma}}^2}{(u - M_{\tilde{e}}^2)(t - M_{\tilde{e}}^2)} \right], \tag{44}
\end{aligned}$$

which is the same result as presented at [38, 39], and also when we put  $M_{\tilde{\gamma}} = 0$  we get Eq.(2) and it is the result presented by Fayet at [37].

Some elementary results from QED are the Møller Scattering [74] (electron-electron scattering) and Bhabha Scattering [75] (electron-positron scattering). The differential cross section to these process are

$$\begin{aligned}\frac{d\sigma}{d\Omega}(e^-e^- \rightarrow e^-e^-) |_{ur} &= \frac{\alpha^2}{4E^2} \left( \frac{1}{\sin^4\theta} + \frac{1}{\cos^4\theta} + 1 \right) , \\ \frac{d\sigma}{d\Omega}(e^-e^+ \rightarrow e^-e^+) |_{ur} &= \frac{\alpha^2}{8E^2} \left( \frac{1 + \cos^4(\theta/2)}{\sin^4(\theta/2)} + \frac{1 + \cos^2\theta}{2} - \frac{2\cos^4(\theta/2)}{\sin^2(\theta/2)} \right) .\end{aligned}\tag{45}$$

The Eqs.(44,45) are obtained in a similar way as we have presented above.

The total cross section to the process  $e^-e^+ \rightarrow \tilde{\gamma}\tilde{\gamma}$  is given by

$$\sigma(e^-e^+ \rightarrow \tilde{\gamma}\tilde{\gamma}) = \frac{2\pi\alpha^2}{s^2} \left\{ \mathcal{S} + 2\Delta\Lambda + \frac{\mathcal{S}\Delta^2}{M_{\tilde{\gamma}}^4 + M_{\tilde{e}}^4 + M_{\tilde{e}}^2(s - 2M_{\tilde{\gamma}}^2)} + 2\frac{M_{\tilde{\gamma}}^2 s \Lambda}{s + 2\Delta} \right\},\tag{46}$$

where

$$\begin{aligned}\mathcal{S} &= \sqrt{s(s - 4M_{\tilde{\gamma}}^2)}, \\ \Delta &= M_{\tilde{e}}^2 - M_{\tilde{\gamma}}^2, \\ \Lambda &= \ln \left[ \frac{s + 2\Delta - \mathcal{S}}{s + 2\Delta + \mathcal{S}} \right].\end{aligned}\tag{47}$$

It is well known that the so called International Linear Collider (ILC) will provide opportunities for both discovery and precision measurements [51]. With the construction of the next generation of  $e^+e^-$  linear colliders, with a center of mass energy up to 1500 GeV and which will be able to operate also in  $\gamma\gamma$ ,  $\gamma e^-$  and  $e^-e^-$  modes, new perspectives arise in detecting new physics beyond the standard model in processes having non-zero initial electric charge (and non-zero lepton number). On the next, where we present our numerical results, we will consider the fotino as being the lightest neutralino of the MSSM.

In the SPS scenarios (see appendix C), the following restriction is satisfied (see Tab.(1))

$$70 \text{ GeV} < M_{\tilde{\gamma}} < 200 \text{ GeV}.\tag{48}$$

This restriction is used in Fig.(11), where we show for three different energies, the behavior of the cross section with the photino and selectron masses, respectively. We get bigger cross section for  $\sqrt{s} = 0.5$  TeV, and the cross section for  $\sqrt{s} = 1$  TeV and  $\sqrt{s} = 1.5$  TeV tend to be closer from each other for heavier fotinos.

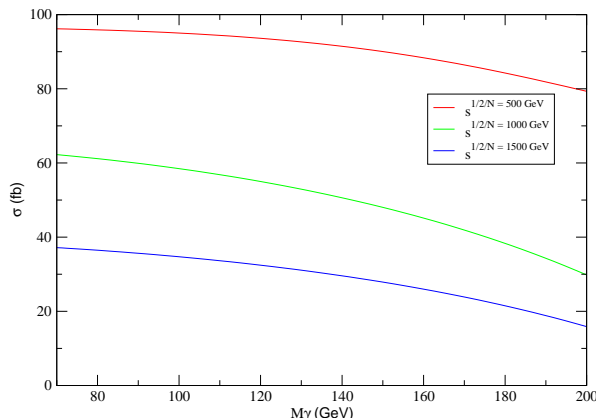


Figure 11: Total cross section of photino production in  $e^-e^+$  collisions as a function of the photino mass for  $\sqrt{s} = 0.5$  TeV (red), for  $\sqrt{s} = 1.0$  TeV (green) and for  $\sqrt{s} = 1.5$  TeV (blue), considering  $M_{\tilde{e}} = 400$  GeV.

## 5 Gluino Production in the MSSM

Gluino and squark production at hadron colliders occurs dominantly via strong interactions. Thus, their production rate may be expected to be considerably larger than for sparticles with just electroweak interactions, whose production was studied at literature.

The cross sections for the production of squarks and gluinos in hadron collisions were calculated at the Born level already quite some time ago [39]. In the present paper we study the gluino production in  $pp$  collisions. We will study the following reactions

$$pp \longrightarrow \tilde{g}\tilde{g}, \tilde{g}\tilde{q} + X \quad (49)$$



in the proton–proton collisions at the “Large Hadron Collider” (LHC).

The leading-order (LO) QCD subprocesses for single gluino production are gluon-gluon and quark-antiquark annihilation ( $gg \rightarrow \tilde{g}\tilde{g}$  and  $q\bar{q} \rightarrow \tilde{g}\tilde{g}$ ), and the Compton process  $qg \rightarrow \tilde{g}\tilde{q}$  (see the subsections below). For double gluino production only the annihilation processes contribute. These two kinds of events could be separated, in principle, by analysing the different decay channels for gluinos and squarks [16, 29].

Incoming quarks (including incoming  $b$  quarks) are assumed to be massless, such that we have  $n_f = 5$  light flavours. We only consider final state squarks corresponding to the light quark flavours. All squark masses are taken equal to  $m_{\tilde{q}}$ <sup>7</sup>. We do not consider in detail top squark production where these assumptions do not hold and which require a more dedicated treatment [76]. In the following subsections we present the calculations for each subprocess discussed above.

## 5.1 Subprocess $\bar{q}q \rightarrow \tilde{g}\tilde{g}$ .

The Feynman diagrams for gluino pair production coming from quark-antiquark initial states are drawn in Figs.(12). In this reaction the Mandelstam variables satisfy the following relation

$$s + t + u = 2M_{\tilde{g}}^2. \quad (50)$$

The kinematic of this reaction is similar to one shown at Fig.(10), with the exchanges  $e^- \rightarrow q$ ,  $e^+ \rightarrow \bar{q}$  and  $\tilde{\gamma} \rightarrow \tilde{g}$ .

The total amplitude to  $\bar{q}q \rightarrow \tilde{g}\tilde{g}$  can be written as

$$\mathcal{M} = \mathcal{M}_s + \mathcal{M}_t + \mathcal{M}_u, \quad (51)$$

where  $|\mathcal{M}|^2$  is the result of averaging over initial spins and colours, and summing over final spins and colours, it means [77, 78]

$$|\mathcal{M}|^2 = \frac{1}{8} \sum_{a,b,c,d,e} \frac{1}{2} \sum_{s_1,s_2} |\mathcal{M}_s + \mathcal{M}_t + \mathcal{M}_u|^2, \quad (52)$$

the sum over spins is similar to that presented in the previous section, and therefore we will not discuss it in detail here, but will only present the results.

---

<sup>7</sup> $L$ -squarks and  $R$ -squarks are therefore mass-degenerate and experimentally indistinguishable.

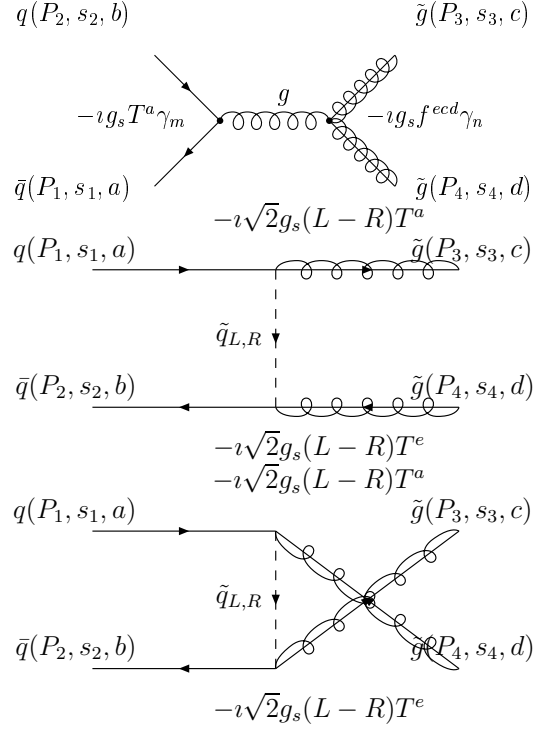


Figure 12: Feynmann diagram to the process  $\bar{q}q \rightarrow \tilde{g}g$ , we fix the orientation for each particle in this reaction as given by the quark in a similar way as we have done previously see Fig.(8).

The mathematical expression to the amplitudes to this process are

$$\begin{aligned}
\mathcal{M}_s &= (-ig_s) \left( w^\dagger(b) \bar{v}(P_2, s_2) T^c \gamma_m w(a) u(P_1, s_1) \right) \left( \frac{g^{mn} \delta^{eg}}{s} \right) (-ig_s) \cdot \\
&\quad \cdot \left( \Omega^\dagger(d) \bar{u}(P_4, s_4) f^{deg} \gamma_n \Omega(e) v(P_3, s_3) \right) \\
&= -\frac{g_s^2}{s} \left( \bar{v}(P_2, s_2) \gamma_m u(P_1, s_1) \right) \left( \bar{u}(P_4, s_4) \gamma^m v(P_3, s_3) \right) \left( w^\dagger(b) T^c w(a) \right) \\
&\quad \cdot f^{deg} \Omega^\dagger(d) \Omega(c). \\
\mathcal{M}_t &= (-i\sqrt{2}g_s(L-R)) \left( w^\dagger(a) \bar{v}(P_1, s_1) T^b \Omega(c) u(P_3, s_3) \right)
\end{aligned}$$

$$\begin{aligned}
& \cdot \left( \frac{i\delta^{be}}{t - M_{\tilde{q}}^2} \right) (-i\sqrt{2}g_s(L - R)) \left( \Omega^\dagger(d)\bar{u}(P_4, s_4)T^e w(f)u(P_2, s_2) \right) \\
& = -\frac{4ig_s^2}{t - M_{\tilde{q}}^2} (\bar{v}(P_2, s_2)u(P_3, s_3)) (\bar{u}(P_4, s_4)u(P_1, s_1)) w^\dagger(a)T^b w(f)\Omega^\dagger(d)T^b\Omega(c) \\
\mathcal{M}_u & = (-i\sqrt{2}g_s(L - R)) \left( w^\dagger(b)\bar{v}(P_2, s_2)T^a\Omega(c)u(P_3, s_3) \right) \\
& \cdot \left( \frac{i\delta^{ae}}{u - M_{\tilde{q}}^2} \right) (-i\sqrt{2}g_s(L - R)) \left( \Omega^\dagger(d)\bar{u}(P_4, s_4)T^e w(f)u(P_1, s_1) \right) \\
& = -\frac{4ig_s^2}{u - M_{\tilde{q}}^2} (\bar{v}(P_2, s_2)u(P_3, s_3)) (\bar{u}(P_4, s_4)u(P_1, s_1)) w^\dagger(b)T^a w(f)\Omega^\dagger(c)T^a\Omega(d).
\end{aligned} \tag{53}$$

where  $w(a)$  and  $\Omega(a)$  are the colour wavefunction to the quarks and gluinos, respectively [30].

In order to calculate the squared total amplitude, see [73]. The squared amplitude is given by

$$|\mathcal{M}|^2 = \frac{1}{16} \sum_{spin} \sum_{cor} |\mathcal{M}_s + \mathcal{M}_t + \mathcal{M}_u|. \tag{54}$$

The colour wavefunction of each quark is given by,  $w(c)$ , and we can show that the following relation is hold

$$\sum_{a,b,c} w_r^\dagger(b)T_{rs}^c w_s(a)w_t^\dagger(a)T_{tu}^c w_u(b) = \sum_{a,b,c} w_u(b)w_r^\dagger(b)T_{rs}^c w_s(a)w_t^\dagger(a)T_{tu}^c. \tag{55}$$

It is easy to show the following relations

$$\begin{aligned}
\sum_b w_u(b)w_r^\dagger(b) &= \delta_{ur}, \\
\sum_a w_s(a)w_t^\dagger(a) &= \delta_{st},
\end{aligned} \tag{56}$$

and therefore the Eq.(55) can be rewritten as

$$\sum_c (T^c)^2 = 4, \tag{57}$$

where  $T^a = \lambda^a/2$  and  $\lambda^a$  are the Gell-Mann matrices (generators of  $SU(3)$  group).

The colour wavefunction of gluinos are  $\Omega(i)$ , where  $i = 1, 2, \dots, 8$ . They are  $8 \times 8$  matrices. These matrices satisfy the following algebra

$$[\Omega(i), \Omega(j)] = \imath f_{ijk} \Omega(k) , \quad (58)$$

where  $f_{ijk}$  are given by the following relation

$$f_{ijk} = -\frac{\imath}{4} \text{Tr}(\lambda_i \lambda_j \lambda_k - \lambda_j \lambda_i \lambda_k) . \quad (59)$$

Therefore the matrix elements of colour wavefunction of gluinos is given by

$$(\Omega(a))_{jk} = -\imath f_{ajk} . \quad (60)$$

We checked our calculations with the ones given by the program FeynArts, Ref.([66]), with the code in the MSSM, Ref([79]). As a final result we get:

$$\begin{aligned} \frac{d\sigma}{dt}(\bar{q}q \rightarrow \tilde{g}\tilde{g}) &= \frac{8\pi\alpha_s^2}{9\hat{s}^2} \left\{ \frac{4}{3} \left( \frac{M_{\tilde{g}}^2 - \hat{t}}{M_{\tilde{q}}^2 - \hat{t}} \right)^2 + \frac{4}{3} \left( \frac{M_{\tilde{g}}^2 - \hat{u}}{M_{\tilde{q}}^2 - \hat{u}} \right)^2 \right. \\ &+ \frac{3}{\hat{s}^2} [(M_{\tilde{g}}^2 - \hat{t})^2 + (M_{\tilde{g}}^2 - \hat{u})^2 + 2M_{\tilde{g}}^2 \hat{s}] \\ &- 3 \left[ \frac{(M_{\tilde{g}}^2 - \hat{t})^2 + M_{\tilde{g}}^2 \hat{s}}{\hat{s}(M_{\tilde{q}}^2 - \hat{t})} \right] - 3 \left[ \frac{(M_{\tilde{g}}^2 - \hat{u})^2 + M_{\tilde{g}}^2 \hat{s}}{\hat{s}(M_{\tilde{q}}^2 - \hat{u})} \right] \\ &\left. + \frac{1}{3} \frac{M_{\tilde{g}}^2 \hat{s}}{(M_{\tilde{q}}^2 - \hat{t})(M_{\tilde{q}}^2 - \hat{u})} \right\} , \end{aligned} \quad (61)$$

this result agrees with those presented at Ref. [39, 29].

## 5.2 Subprocess $gg \rightarrow \tilde{g}\tilde{g}$ .

The Feynman diagrams for gluino production coming from gluon fusion are drawn in Fig.(13). The total amplitude (the Mandelstam variables are related as shown at Eq.(50)) is given by

$$\mathcal{M} = \mathcal{M}_s + \mathcal{M}_t + \mathcal{M}_u, \quad (62)$$

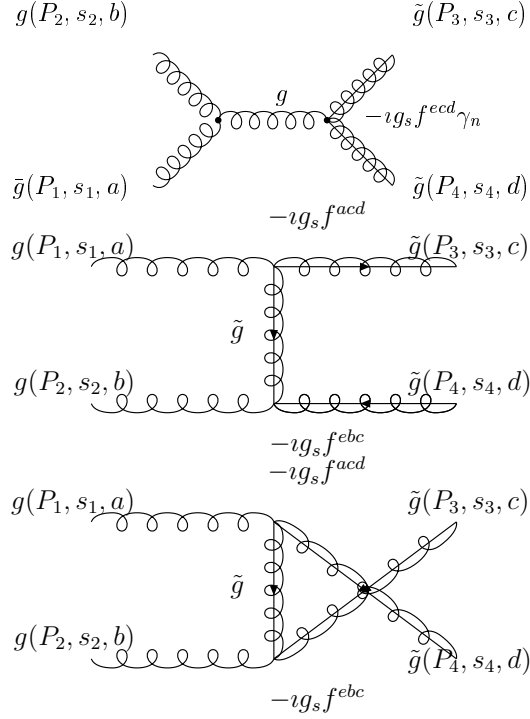


Figure 13: Feynman diagrams for gluino pair production came from gluon-gluon initial states, the fermion flow is indicated by the arrows.

where

$$\begin{aligned}
\mathcal{M}_s &= (-ig_s f^{abe}) \left( \epsilon_m(P_1) a^a(c) \epsilon_n^*(c) a^b(c) \right) \left( \frac{g^{mn} \delta^{ef}}{s} \right) (-ig_s f^{cdf}) \left( \Omega^\dagger(c) \bar{u}(P_3) \Omega(d) u(P_4) \right) \\
&\quad \cdot [g_{mn}(P_1 - P_2)_r + g_{nr}(P_2 + Q)_m - g_{rm}(Q + P_1)_r] \\
\mathcal{M}_t &= (-ig_s f^{bde}) \left( \epsilon_m(P_2) a^b(c) u(P_4) \Omega(d) \right) \left( \frac{i(\not{A} + M_{\tilde{g}})}{t - M_{\tilde{g}}^2} \delta^{de} g^{mn} \right) (-ig_s f^{bcf}) \\
&\quad \cdot (\epsilon_n(P_1) a^a(c) u(P_3) \Omega(c)) \\
\mathcal{M}_u &= (-ig_s f^{bce}) \left( \epsilon_m(P_2) a^b(c) u(P_3) \Omega(c) \right) \left( \frac{i(\not{A} + M_{\tilde{g}})}{u - M_{\tilde{g}}^2} \delta^{de} g^{mn} \right) (-ig_s f^{bdf}) \\
&\quad \cdot (\epsilon_n(P_1) a^a(c) u(P_4) \Omega(d)) .
\end{aligned} \tag{63}$$

Using Eq.(63) at Eq.(62) and using the FeynCalc we obtain:

$$\begin{aligned}
\frac{d\sigma}{d\hat{t}}(gg \rightarrow \tilde{g}\tilde{g}) &= \frac{9\pi\alpha_s^2}{4\hat{s}^2} \left\{ \frac{2(M_g^2 - \hat{t})(M_g^2 - \hat{u})}{\hat{s}^2} + \frac{(M_g^2 - \hat{t})(M_g^2 - \hat{u}) + 2M_g^2(M_g^2 + \hat{t})}{(M_g^2 - \hat{t})^2} \right. \\
&+ \frac{(M_g^2 - \hat{t})(M_g^2 - \hat{u}) + 2M_g^2(M_g^2 + \hat{u})}{(M_g^2 - \hat{u})^2} + \frac{M_g^2(\hat{s} - 4M_g^2)}{(M_g^2 - \hat{t})(M_g^2 - \hat{u})} \\
&+ \left. \frac{(M_g^2 - \hat{t})(M_g^2 - \hat{u}) + M_g^2(\hat{u} - \hat{t})}{\hat{s}(M_g^2 - \hat{t})} + \frac{(M_g^2 - \hat{t})(M_g^2 - \hat{u}) + M_g^2(\hat{u} - \hat{t})}{\hat{s}(M_g^2 - \hat{u})} \right\}, \tag{64}
\end{aligned}$$

again in agreement with the results presented at Ref. [39, 29].

### 5.3 Subprocess $qg \rightarrow \tilde{q}\tilde{g}$ .

The Feynman diagrams for gluino production coming from the Compton scattering  $qg$  are drawn at Fig.(14). In this case the Mandelstam variables satisfy

$$s + t + u = M_g^2 + M_{\tilde{q}}^2. \tag{65}$$

The total cross section is

$$\mathcal{M} = \mathcal{M}_s + \mathcal{M}_t + \mathcal{M}_u, \tag{66}$$

where

$$\begin{aligned}
\mathcal{M}_s &= (-i\sqrt{2}g_s(L - R)) \left( w^\dagger(d)T^f w(c)u(P_3, s_3) \right) \left( \frac{i(\not{A} + M_{\tilde{g}})}{s} \delta^{fe} \right) (-ig_s f^{eac}) \cdot \\
&\cdot \left( \Omega^\dagger(a)\bar{u}(P_1, s_1) \right) T^e \gamma^m \epsilon^n(P_2) a^e(b) \\
\mathcal{M}_t &= (-i\sqrt{2}g_s(L - R)) \left( w^\dagger(d)T^f w(b)u(P_2, s_2) \right) \left( \frac{i(\not{A} + M_{\tilde{g}})}{t - M_{\tilde{g}}^2} \delta^{fe} \right) (-ig_s f^{eac}) \cdot \\
&\cdot (\epsilon^\mu(P_1) a^e(a) \gamma^\mu u(P_3, s_3)) \Omega(c) \\
\mathcal{M}_u &= (-i\sqrt{2}g_s(L - R)) \left( w^\dagger(d)T^f w(b)u(P_3, s_3) \right) \left( \frac{i(\not{A} + M_{\tilde{g}})}{u - M_{\tilde{g}}^2} \delta^{fe} \right) (-ig_s f^{eac}) \cdot \\
&\cdot (\epsilon^\mu(P_1) a^e(a) \gamma^\mu u(P_4, s_4)) \Omega(c). \tag{67}
\end{aligned}$$

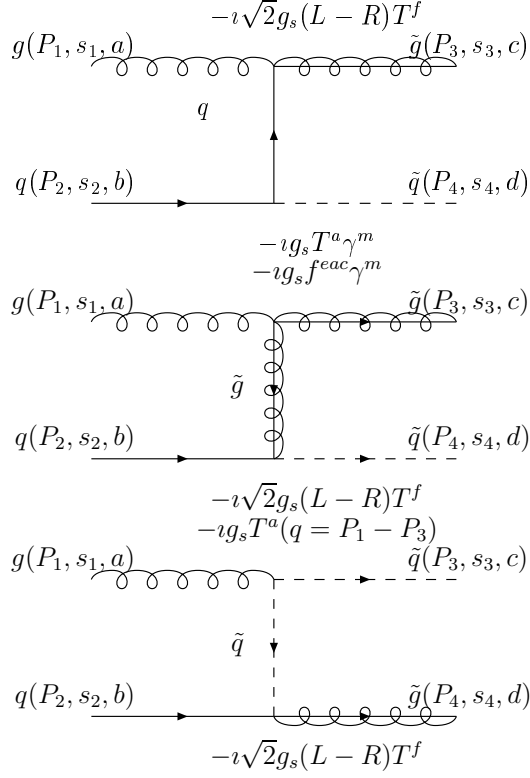


Figure 14: Feynman diagrams for squark–gluino production, the fermion flow is indicated by the arrows.

The differential cross section for this reaction is given by

$$\begin{aligned}
\frac{d\sigma}{d\hat{t}}(qg \rightarrow \tilde{q}\tilde{g}) &= \frac{\pi\alpha_s^2}{24\hat{s}^2} \left\{ \left[ \frac{\frac{16}{3}(\hat{s}^2 + (M_{\tilde{q}}^2 - \hat{u})^2) + \frac{4}{3}\hat{s}(M_{\tilde{q}}^2 - \hat{u})}{\hat{s}(M_{\tilde{g}}^2 - \hat{t})(M_{\tilde{g}}^2 - \hat{u})} \right] \right. \\
&\times \left. \left( (M_{\tilde{g}}^2 - \hat{u})^2 + (M_{\tilde{q}}^2 - M_{\tilde{g}}^2)^2 + \frac{2\hat{s}M_{\tilde{g}}^2(M_{\tilde{q}}^2 - M_{\tilde{g}}^2)}{(M_{\tilde{g}}^2 - \hat{t})} \right) \right\}, \tag{68}
\end{aligned}$$

in agreement with Ref. [39, 29].

The total cross section for the gluino production can be obtained by adding Eqs.(61, 64, 68). By doing this, we reproduce the results presented

at [39, 80]. We have used these expressions to get the results presented at [32, 73, ?, 81].

The main aim of the Large Hadron Collider (LHC) [52], which is already running and soon will be in complete operation with 14 TeV, is to find the Higgs particle. That discovery may either confirm the Standard Model (SM) or open new windows towards new physics. This machine will also study collisions involving nuclei - pA (proton-nucleus,  $\sqrt{s} = 8.8 \text{ TeV}$ ) and AA (nucleus-nucleus,  $\sqrt{s} = 5.5 \text{ TeV}$ ) LHC modes. Results for gluino production in the pA and AA modes were presented for the first time in the Refs.[73, 81].

Before we present our numerical results and plots about the gluino production at the LHC, it is important to stress that gluon fluxes and large color factors make gluon-gluon ( $gg$ ) fusion contributions dominants at LHC energies if  $M_{\tilde{g}}, M_{\tilde{q}} \leq 1 \text{ TeV}$ , while reactions involving valence quarks dominate gluino production at the Tevatron in the allowed mass range. The rate of gluino pair production reaches the highest values when  $M_{\tilde{g}} \simeq M_{\tilde{q}}$  [16].

In Fig.15 we present the LO QCD total cross section for gluino production at the LHC as a function of the gluino masses. We use the CTEQ6L [82], parton densities, with two assumptions on the squark masses and choices of the hard scale (curves). The sensitivity with the hard scale is also presented in the case  $m_{\tilde{q}} = m_{\tilde{g}}$ . We also, want to stress that the behaviour of our curves are similar to ones presented at Chapter 12 on reference [29], where they use the CTEQ5L parton distribution on their calculation.

Since the  $pp$  CM energy  $\sqrt{s} = 14 \text{ TeV}$  is several times larger than the expected gluino and squark masses, these particles might be produced and detected at the LHC.

## 6 Gluino decays

We know that the gluinos are unstable particles, and the main decay channels are ([16, 29])

$$\tilde{g} \rightarrow q\bar{q}\tilde{\chi}_1^0 \quad (69)$$

$$\tilde{g} \rightarrow q\bar{q}'\tilde{\chi}_1^\pm \quad (70)$$

$$\tilde{g} \rightarrow g\tilde{\chi}_1^0, \quad (71)$$

and some corresponding experimental SUSY signatures at LHC are shown in Figs. 16 and 17.



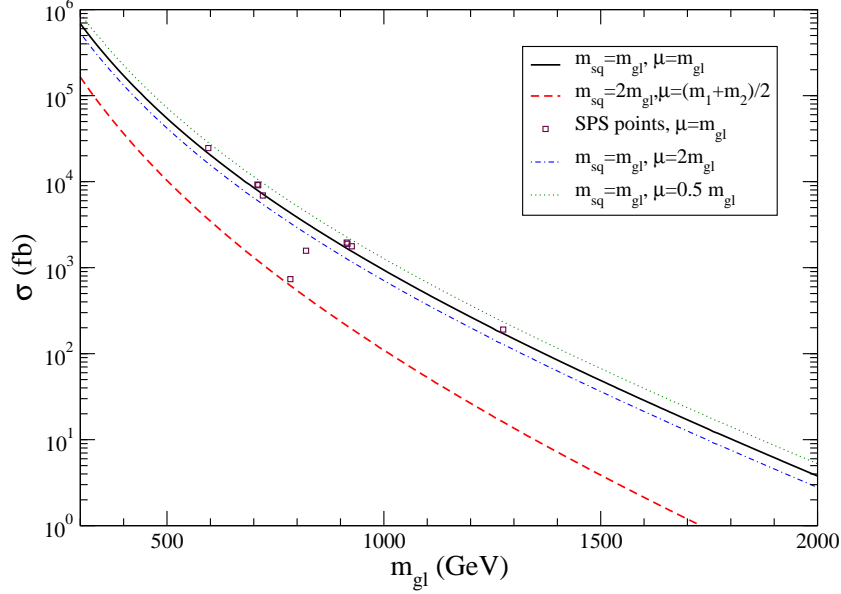


Figure 15: The total LO cross section for gluino production at the LHC as a function of the gluino masses. Parton densities: CTEQ6L, with two assumptions on the squark masses and choices of the hard scale (curves). The sensitivity with the hard scale is also presented in the case  $m_{\tilde{q}} = m_{\tilde{g}}$ . The points are the numerical results for the SPS points as explained in the text.

## 7 Conclusion

On this article, we first presented as to get Feynman amplitudes when we deal with Majorana fermions. The method is based on a well-defined fermion flow and we have vertices equations without explicit charge-conjugation matrices. We can use this formalism when we perform calculations with Majorana neutrinos, leptogenesis and in SUSY phenomenology. Later, we review how to calculate the photino and gluino production. We hope that this review will be useful to those entering the field of supersymmetric extensions of the standard model.

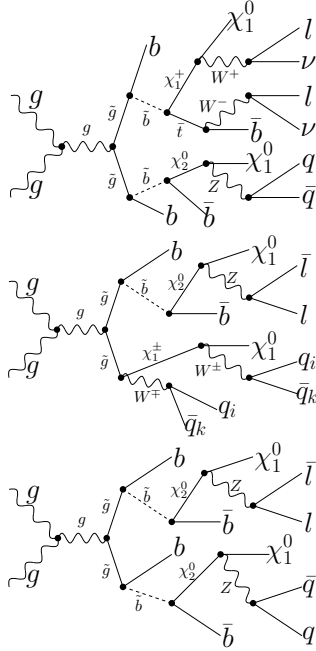


Figure 16: Creation of the pair of gluino with further cascade decay, first decay  $\rightarrow 2l \ 2\nu \ 6j \ \cancel{E}_T$ , second decay  $\rightarrow 2l \ 6j \ \cancel{E}_T$ , third decay  $\rightarrow 2l \ 6j \ \cancel{E}_T$ , take from Ref. [83].

## Acknowledgments

This work was supported by CNPq, DBE supported by Master quota of CNPq from IF-UFRGS. We are grateful to Pierre Fayet to give us several interesting information about the photino and gluino phenomenology.

## A Feynman rules for SQED

The Supersymmetric Quantum Electrodynamics (SQED) is the supersymmetric generalization of QED [15, 16, 17]. The physical spectrum of this model is given by the positron, electron, photon, spositron, selectron and photino.

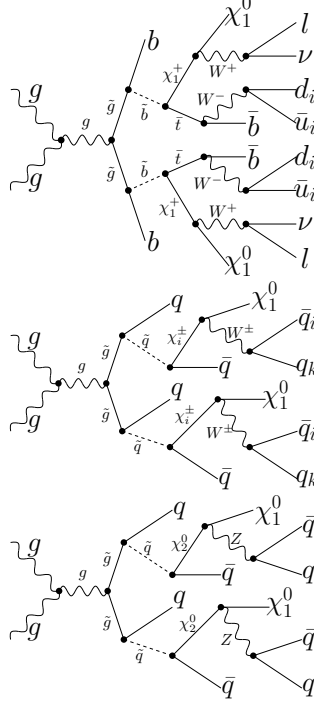


Figure 17: Creation of the pair of gluino with further cascade decay, first decay  $\rightarrow 2l \ 2\nu \ 8j \ \cancel{E}_T$ , second decay  $\rightarrow 8j \ \cancel{E}_T$ , third decay  $\rightarrow 8j \ \cancel{E}_T$ , take from Ref. [83].

In order to introduce all these particles, we must introduce two chirals superfields  $\Phi_+$ ,  $\Phi_-$ , containing the left fermion field and the right fermion fields, respectively, plus one vectorial superfield  $V$ , where we introduce the photon, giving the following expressions

$$\begin{aligned}
\Phi_+(y, \theta) &= \phi_+(y) + \sqrt{2}\theta\xi_+(y) + \theta\theta F_+(y), \\
\Phi_-(y, \theta) &= \phi_-(y) + \sqrt{2}\theta\xi_-(y) + \theta\theta F_-(y), \\
V_{WZ}(y, \theta, \bar{\theta}) &= -\theta\sigma^m\bar{\theta}v_m(y) + i\theta\theta\bar{\theta}\bar{\lambda}(y) - i\bar{\theta}\bar{\theta}\theta\lambda(y) + \frac{1}{2}\theta\theta\bar{\theta}\bar{\theta}(D(y) - i\partial_m v^m(y)),
\end{aligned} \tag{72}$$

where the subscript  $WZ$  means that the vectorial superfield is written at Wess-Zumino gauge. The fields  $\phi_+$  and  $\phi_-$  are the spositrons and selectrons, respectively, while  $\xi_+$  and  $\xi_-$  will form the positron and the electron. The photon is given by  $v_m$ , while their supersymmetric partner, the photino, is given by  $\lambda$ , and the  $F$  and  $D$  terms are auxiliary fields necessary to close the SUSY algebra.

The superfields given at Eq.(72) satisfy the following transformation law

$$\begin{aligned}\Phi'_+ &= e^{-2ie\Lambda}\Phi_+ , \\ \Phi'_- &= e^{2ie\Lambda}\Phi_- , \\ V' &= V + \imath(\Lambda - \Lambda^+) ,\end{aligned}\tag{73}$$

where  $\Lambda$  is a chiral superfield and  $e$  and  $-e$  are the electric charge of  $\Phi_+$  and  $\Phi_-$  respectively.

The supersymmetric lagrangian of SQED in terms of the superfields is given by

$$\begin{aligned}\mathcal{L}_{SQED} &= \frac{1}{4} \left( \int d^2W^\alpha W_\alpha + \int d^2\bar{W}^{\dot{\alpha}} \bar{W}_{\dot{\alpha}} \right) + \int d^4\theta \bar{\Phi}_+ e^{2eV} \Phi_+ + \int d^4\theta \bar{\Phi}_- e^{2eV} \Phi_- \\ &+ M \left( \int d^2\theta \Phi_+ \Phi_- + \int d^2\bar{\theta} \bar{\Phi}_+ \bar{\Phi}_- \right) .\end{aligned}\tag{74}$$

This Lagrangian is manifestly gauge invariant and conserves  $R$ -parity (therefore sparticles appear in pairs (or quartet) at any vertex, it means we can have  $e^-e^- \rightarrow \tilde{e}^-\tilde{e}^-$  but we can not have  $e^-e^- \rightarrow e^-\tilde{e}^-$  because it violate  $R$ -parity) [16].

Next we can define the following four component Dirac spinor to the electron as

$$\Psi = \begin{pmatrix} \xi_+ \\ \xi_- \end{pmatrix} ,\tag{75}$$

while for the photinos we define the following four component Majorana spinor

$$\Lambda_M = \begin{pmatrix} \lambda \\ \bar{\lambda} \end{pmatrix} .\tag{76}$$

The full lagrangian of this model in terms of the physical fields can be found in the following Refs. [15, 16]. The interaction Lagrangian of SQED is

given by

$$\begin{aligned}
\mathcal{L}_{intQED} = & e\bar{\Psi}\gamma^m\Psi v_m - e^2 \left( \overline{\phi_+}\phi_+\overline{\phi_+}\phi_+ + \overline{\phi_-}\phi_-\overline{\phi_-}\phi_- + 2\overline{\phi_+}\phi_+\overline{\phi_-}\phi_- \right) \\
& - ie\sqrt{2} \left( \bar{\Psi}L\Lambda_M\phi_+ + \bar{\Psi}R\Lambda_M\phi_- + hc \right) - e^2 \left( \overline{\phi_+}\phi_+ + \overline{\phi_-}\phi_- \right) v_mv^m .
\end{aligned} \tag{77}$$

From Eq.(77) we may pick the Feynman rules we have used in this article. The vertices we have used in this articles are:

- electron-electron-photon vertex:  $-ie\gamma^m$ ;
- right-handed electron-photino-selectron vertex:  $-ie\sqrt{2}R$ ;
- left-handed electron-photino-selectron vertex:  $-ie\sqrt{2}L$ .

These vertices are shown at Fig.(18).

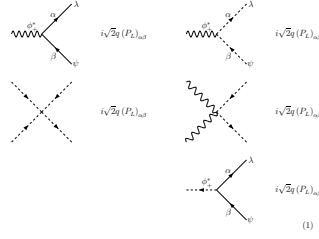


Figure 18: Feynman Rules of SQED taken from Eq.(77).

## B Feynman rules for SQCD

The Feynman rules of SQCD can be found in the following Refs. [15, 16, 22, 32]. Here we only cite them

- quark-quark-gluon vertex:  $-ig_s T_{rs}^a \gamma^m$ ;
- gluino-gluino-gluon vertex:  $-ig_s f^{bac} \gamma^m$ ;
- squark-squark-gluon vertex:  $-ig_s T_{rs}^a (k_i + k_j)^m$ ;

- squark-gluon-gluon vertex:  $-ig_s^2 \left( \frac{\delta_{ab}\delta_{rt}}{3} + d^{abc}T_{rt}^c \right) g_{mn};$
- gluino-quark-squark vertex:  $-i\sqrt{2}g_s(L - R)T_{rs}^a.$

## C Masses of Gluinos, squarks, fotinos and selectrons

The “Snowmass Points and Slopes” (SPS) [69] are a set of benchmark points and parameter lines in the MSSM parameter space corresponding to different scenarios in the search for supersymmetry at present and future experiments (See [70] for a very nice review). The aim of this convention is reconstructing the fundamental supersymmetric theory, and its breaking mechanism, from the experimental data. The points SPS 1-6 are Minimal Supergravity (mSUGRA) model, SPS 7-8 are gauge-mediated supersymmetry breaking (GMSB) model, and SPS 9 are anomaly-mediated supersymmetry breaking (mAMSB) model [69, 70, 71]. Therefore in several scenarios, given at SPS convention, the neutralinos (photinos) are the lighter particle while the gluino is the most massive particle of the MSSM.

Each set of parameters leads to different masses of the gluinos, squarks, fotinos and selectrons, which are the only relevant parameters in our study, and we shown their values in Tab.(1).

## References

- [1] S.J. L. Rosner, *Am. J. Phys.* **71**, 302, (2003); A. S. Kronfeld and C. Quigg, *Am. J. Phys.* **78**, 1081, (2010).
- [2] SuperK, Y. Fukuda *et al.*, *Phys. Rev. Lett.* **81**, 1562, (1998); **82**, 2644, (1999); **85**, 3999, (2000); **86**, 5651, (2001); Y. Suzuki, *Nucl. Phys. B (Proc. Suppl.)* **77**, 35, (1999); SuperK, Y. Fukuda *et al.*, *Phys. Rev. Lett.* **81**, 1158, (1998); **82**, 1810, (1999); Y. Suzuki, *Nucl. Phys. B (Proc. Suppl.)* **77**, 35, (1999); S. Fukuda *et al.*, *Phys. Rev. Lett.* **86**, 5651, (2001).
- [3] KamLAND Collaboration, K. Eguchi *et al.*, *Phys. Rev. Lett.* **90**, 021802, (2003); T. Araki *et al.*, *Phys. Rev. Lett.* **94**, 081801, (2005).

Scenario	$m_{\tilde{g}} (GeV)$	$m_{\tilde{q}} (GeV)$	$m_{\tilde{\gamma}} (GeV)$	$m_{\tilde{e}} (GeV)$
SPS1a	595.2	539.9	96	202
SPS1b	916.1	836.2	96	202
SPS2	784.4	1533.6	79	1456
SPS3	914.3	818.3	160	287
SPS4	721.0	732.2	118	448
SPS5	710.3	643.9	119	256
SPS6	708.5	641.3	189	264
SPS7	926.0	861.3	161	261
SPS8	820.5	1081.6	137	356
SPS9	1275.2	1219.2	175	319

Table 1: The values of the masses of gluinos, squarks, fotinos and selectrons in the SPS scenarios.

- [4] SNO Collaboration, Q. R. Ahmad *et al.*, *Phys. Rev. Lett.***89**, 011301, (2002); **89**, 011302, (2002); **92**, 181301, (2004); B. Aharmim *et al.*, *Phys. Rev.***C72**, 055502, (2005).
- [5] B. Kayser, *J. Phys. Conf. Ser.* **173**, 012013, (2009).
- [6] R. N. Mohapatra *et al.*, *Rept. Prog. Phys.***70**, 1757, (2007).
- [7] N. F. Bell, *J. Phys. Conf. Ser.***136**, 022043, (2008).
- [8] P. B. Pal, arXiv:1006.1718 [hep-ph].
- [9] G. Cvetič, Claudio Dib, Sin Kyu Kang, C. S. Kim, arXiv:1005.4282.
- [10] S. S. C. Law, arXiv:0901.1232 [hep-ph].
- [11] S. S. C. Law, *Mod. Phys. Lett.***A25**, 994, (2010).
- [12] Yu. A. Gol’fand and E.P. Likhtman, *ZhETF Pis. Red.***13**, 452, (1971) [*JETP Lett.***13**, 323, (1971)].

- [13] D.V. Volkov and V.P. Akulov, *Phys. Lett.***B46**, 109, (1973).
- [14] J. Wess and B. Zumino, *Nucl. Phys.***B70**, 39, (1974); *Phys. Lett.***B49**, 52, (1974); *Nucl. Phys.***B78**, 1, (1974).
- [15] J. Wess and J. Bagger, *Supersymmetry and Supergravity* Second Edition, Princeton University Press, Princeton NJ, (1992).
- [16] M. Drees, R. M. Godbole and P. Roy, *Theory and Phenomenology of Sparticles* First Edition, World Scientific Publishing Co. Pte. Ltd., Singapore, (2004).
- [17] H. J. W. Müller-Kirsten and A. Wiedemann, *SUPERSYMMETRY: AN INTRODUCTION WITH CONCEPTUAL AND CALCULATIONAL DETAILS*, Second Edition, World Scientific Publishing Co. Pte. Ltd., Singapore, (2010).
- [18] P. Fayet, *Nucl. Phys.***B90**, 104, (1975).
- [19] P. Fayet, *Phys. Lett.***B64**, 159, (1976); **B69**, 489, (1977).
- [20] P. Fayet, *Phys. Lett.***B70**, 461, (1977).
- [21] P. Fayet, *Nucl. Phys. Proc. Suppl.***101**, 81, (2001) (Also in \*Minneapolis 2000, 30 years of supersymmetry\* 81-98); P. Fayet, arXiv:hep-ph/0104302 (Contribution to 'The Supersymmetric World - The Beginnings of the The Theory' G. Kane and M. Shifman, eds. (World Scientific, 2000), p. 120. In \*Kane, G.L. (ed.) et al.: The supersymmetric world\* 120-144); P. Fayet, arXiv:hep-ph/9912413 (Contribution to the Yuri Golfand Memorial Volume, M. Shifman, ed., World Scientific. In \*Shifman, M.A. (ed.): The many faces of the superworld\* 476-497).
- [22] M. C. Rodriguez, *Int. J. Mod. Phys.***A25**, 1091, (2010).
- [23] H. Goldberg, *Phys. Rev. Lett.***50**, 1419, (1983).
- [24] P. Fayet, *Phys. Lett.* **B86**, 272, (1979).
- [25] G.R. Farrar and P. Fayet, *Phys. Lett.* **B76**, 575, (1978).
- [26] G.R. Farrar and P. Fayet, *Phys. Lett.* **B79**, 442, (1978).



- [27] E. Cremmer, P. Fayet and L. Girardello, *Phys. Lett.***B122**, 41, (1983).
- [28] D. Bailin and A. Love, *Supersymmetric Gauge Field Theory and String Theory*, First Edition, Institute of Physics Publishing, Bristol UK, (1994).
- [29] H. Baer and X. Tata, *Weak Scale Supersymmetry*, First Edition, Cambridge University Press, United Kindom, (2006).
- [30] I. Aitchison, *Supersymmetry in Particle Physics: An Elementary Introduction*, First Edition, Cambridge University Press, United Kindom, (2007).
- [31] D. J. H. Chung, L. L. Everett, G. L. Kane, S. F. King, J. D. Lykken and L. T. Wang, *Phys.Rept.***407**, 1, (2005).
- [32] C. B. Mariotto and M. C. Rodriguez, *Braz. J. Phys.***38**, 503, (2008) and arXiv:0805.2094 [hep-ph].
- [33] P. Nath and R. Arnowitt, *Phys. Lett.***B56**, 177, (1975); D. Z. Freedman, P. van Nieuwenhuizen and S. Ferrara, *Phys. Rev.***D13**, 3214, (1976); S. Deser and B. Zumino, *Phys. Lett.***B62**, 335, (1976); see also "Supersymmetry", S.Ferrara, ed. (North Holland/World Scientific, Amsterdam/Singapore, 1987).
- [34] U. Amaldi, W. de Boer, H. Fürstenau, *Phys. Lett.***B260**, 447, (1991).
- [35] K. Inoue, A. Komatsu and S. Takeshita, *Prog. Theor. Phys.* **68**, 927, (1982); *Prog. Theor. Phys.* **70**, 330, (1983).
- [36] V. Barger, M. S. Berger and P. Ohmann, *Phys. Rev.* **D47**, 1093, (1993); W. de Boer, R. Ehret and D. Kazakov, *Z. Phys.***C67**, 647, (1995); W. de Boer et al., *Z. Phys.* **C71**, 415, (1996).
- [37] P. Fayet, *Phys. Lett.***B117**, 460, (1982).
- [38] H.E. Haber and G.L. Kane, *Phys. Rep.***117**, 75, (1975).
- [39] S. Dawson, E. Eichten and C. Quigg, *Phys. Rev.***D31**, 1581, (1985).
- [40] T. Kobayashi and M. Kuroda, *Phys. Lett.***B139**, 208, (1984).

- [41] K. Grassie and P. N. Pandita, *Phys. Rev.***D30**, 22, (1984).
- [42] J. D. Ware and M. E. Machacek, *Phys. Lett.***B142**, 300, (1984).
- [43] L. Bento, J. C. Romao and A. Barroso, *Phys. Rev.***D33**, 1488, (1986).
- [44] V. S. Berezinsky, E. V. Bugaev and E. S. Zaslavskaya, *Nucl. Phys.***B272**, 193, (1986).
- [45] H. E. Haber and G. L. Kane, *Nucl. Phys.***B232**, 333, (1984).
- [46] H. Baer, V. D. Barger, D. Karatas and X. Tata, *Phys. Rev.***D36**, 96, (1987).
- [47] H. Baer, X. Tata and J. Woodside, *Phys. Rev.***D42**, 1568, (1990).
- [48] H. E. Haber and G. L. Kane, *Nucl. Phys.***B232**, 333, (1984).
- [49] E. Ma and G. G. Wong, *Mod. Phys. Lett.* **A3**, 1561, (1988).
- [50] R. Barbieri, G. Gamberini, G. F. Giudice and G. Ridolfi, *Nucl. Phys.***B301**, 15, (1988).
- [51] <http://www.linearcollider.org/>
- [52] <http://lhc.web.cern.ch/lhc/>
- [53] A. D. Sakharov, *Pisma Zh. Eksp. Teor. Fiz.* **5**, 32 (1967) [*JETP Lett.* **5**, 24 (1967 SOPUA,34,392-393.1991 UFNAA,161,61-64.1991)].
- [54] M. Kobayashi and T. Maskawa, *Prog. Theor. Phys.* **49**, 652 (1973).
- [55] M. B. Gavela, P. Hernandez, J. Orloff and O. Pene, *Mod. Phys. Lett.* **A 9**, 795 (1994) [arXiv:hep-ph/9312215].
- [56] P. Minkowski, *Phys. Lett. B* **67**, 421 (1977); T. Yanagida, in *Workshop on Unified Theories*, KEK report 79-18 p.95 (1979); M. Gell-Mann, P. Ramond, R. Slansky, in *Supergravity* (North Holland, Amsterdam, 1979) eds. P. van Nieuwenhuizen, D. Freedman, p.315; S. L. Glashow, in *1979 Cargese Summer Institute on Quarks and Leptons* (Plenum Press, New York, 1980) eds. M. Levy, J.-L. Basdevant, D. Speiser, J. Weyers, R. Gastmans and M. Jacobs, p.687; R. Barbieri, D. V. Nanopoulos,

- G. Morchio and F. Strocchi, *Phys. Lett. B* **90**, 91 (1980); R. N. Mohapatra and G. Senjanovic, *Phys. Rev. Lett.* **44**, 912 (1980).
- [57] M. Fukugita and T. Yanagida, *Phys. Lett. B* **174**, 45 (1986).
  - [58] R. Barbier *et al.*, *Phys. Rept.***420**, 1, (2005).
  - [59] G. Moreau, arXiv:hep-ph/0012156.
  - [60] H. Dreiner, arXiv:hep-ph/9707435.
  - [61] E.I. Gates, and K. L. Kowalski, *Phys. Rev.***D45**, 1693, (1992).
  - [62] A. Denner, H. Eck, O. Hahn and J. Küblbeck, *Nucl. Phys.***B387**, 467, (1992).
  - [63] A. Denner, H. Eck, O. Hahn and J. Küblbeck, *Phys. Lett.***B387**, 278, (1992).
  - [64] M. Srednicki, *Quantum field theory*, Fourth Edition, Cambridge University Press, United Kindom, (2010) and also available at arXiv:hep-th/0409035 and arXiv:hep-th/0409036.
  - [65] N. F. Bell, B. Kayser and S. S. C. Law, *Phys. Rev.***D78**, 085024, (2008).
  - [66] T. Hahn, *Comput. Phys. Commun.***140**, 418, (2001).
  - [67] A. Bartl, H. Fraas, W. Majerotto and N. Oshimo, *Phys. Rev.***D40**, 1594, (1989).
  - [68] M. S. Carena and C. E. M. Wagner, *Phys. Lett.* **B195**, 599, (1987).
  - [69] B.C. Allanach *et al.*, *Eur.Phys.J.***C25**, 113, (2002).
  - [70] Nabil Ghodbane and Hans-Ulrich Martyn, hep-ph/0201233.
  - [71] <http://spa.desy.de/spa/>
  - [72] K. A. Olive and S. Rudaz, *Phys. Lett.***B340**, 74, (1994).
  - [73] D.B. Espindola, "Produção de Fotinos e Gluínos nas Extensões Supersimétricas da Eletrodinâmica Quântica e da Cromodinâmica Quântica", Master thesis defended at 03/18/2010.

- [74] C. Møller, *Ann. Phys.***14**, 531, (1932).
- [75] H. J. Bhabha, *Proc. Roy. Soc.***A154**, 195, (1935).
- [76] W. Beenakker, M. Krämer, T. Plehn, M. Spira and P. M. Zerwas, *Nucl. Phys.***B515**, 3, (1998).
- [77] I. J. R. Aitchison and A. J. G. Hey, “Gauge theories in particle physics: A practical introduction. Vol. 1: From relativistic quantum mechanics to QED,” *Bristol, UK: IOP Publishing*.
- [78] I. J. R. Aitchison and A. J. G. Hey, “Gauge theories in particle physics: A practical introduction. Vol. 2: From QCD and Electroweak Theory,” *Bristol, UK: IOP Publishing*.
- [79] T. Hahn and C. Schappacher, *Comput. Phys. Commun.* **143**, 54, (2002).
- [80] W. Beenakker, R. Höpker, M. Spira and P.M. Zerwas, *Nucl. Phys.***B492**, 51, (1997).
- [81] C. Brenner Mariotto, D. B. Espindola and M. C. Rodriguez, “Gluino production in ultrarelativistic heavy ion collisions and nuclear shadowing”, *Phys. Rev.* **C83**, 064902 (2011).
- [82] J. Pumplin, D. R. Stump, J. Huston, H. L. Lai, P. Nadolsky and W. K. Tung, *JHEP***0207**, 012, (2002).
- [83] A. V. Gladyshev and D. I. Kazakov, *Phys. Atom. Nucl.***70**, 1553, (2007).